Accepted Manuscript

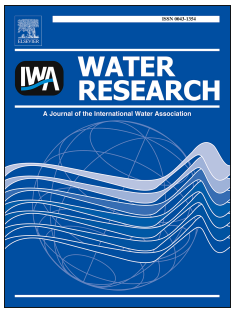

Recent Advances in Mathematical Modeling of Nitrous Oxides Emissions from Wastewater Treatment Processes

Dr. Bing-Jie Ni, Zhiguo Yuan

PII: S0043-1354(15)30261-X

DOI: 10.1016/j.watres.2015.09.049

Reference: WR 11557

To appear in: *Water Research*

Received Date: 25 June 2015

Revised Date: 27 September 2015

Accepted Date: 28 September 2015

Please cite this article as: Ni, B.-J., Yuan, Z., Recent Advances in Mathematical Modeling of Nitrous Oxides Emissions from Wastewater Treatment Processes, *Water Research* (2015), doi: 10.1016/j.watres.2015.09.049.

This is a PDF file of an unedited manuscript that has been accepted for publication. As a service to our customers we are providing this early version of the manuscript. The manuscript will undergo copyediting, typesetting, and review of the resulting proof before it is published in its final form. Please note that during the production process errors may be discovered which could affect the content, and all legal disclaimers that apply to the journal pertain.

ACCEPTED MANUSCRIPT

Recent Advances in Mathematical Modeling of Nitrous Oxides Emissions from Wastewater Treatment Processes

Bing-Jie Ni,* Zhiguo Yuan

Advanced Water Management Centre, The University of Queensland, St. Lucia, Brisbane, Queensland 4072, Australia

***Corresponding author:** Dr. Bing-Jie Ni, Phone: + 61 7 3346 3219, Fax: +61 7 3365 4726, E-mail: b.ni@uq.edu.au

Abstract:

Nitrous oxide (N_2O) can be emitted from wastewater treatment contributing to its greenhouse gas footprint significantly. Mathematical modeling of N_2O emissions is of great importance toward the understanding and reduction of the environmental impact of wastewater treatment systems. This article reviews the current status of the modeling of N_2O emissions from wastewater treatment. The existing mathematical models describing all the known microbial pathways for N_2O production are reviewed and discussed. These included N_2O production by ammonia-oxidizing bacteria (AOB) through the hydroxylamine oxidation pathway and the AOB denitrification pathway, N_2O production by heterotrophic denitrifiers through the denitrification pathway, and the integration of these pathways in single N_2O models. The calibration and validation of these models using lab-scale and full-scale experimental data is also reviewed. We conclude that the mathematical modeling of N_2O production, while is still being enhanced supported by new knowledge development, has reached a maturity that facilitates the estimation of site-specific N_2O emissions and the

development of mitigation strategies for a wastewater treatment plant taking into the specific design and operational conditions of the plant.

Keywords: AOB, model, nitrous oxide, hydroxylamine oxidation, AOB denitrification, heterotrophic denitrification

1. Introduction

Nitrous oxide (N_2O) not only is a significant greenhouse gas, with an approximately 300-fold stronger warming effect than carbon dioxide (IPCC, 2007), but also reacts with ozone in the stratosphere leading to ozone layer depletion (Portmann et al., 2012). It can be produced and directly emitted from wastewater treatment systems (Foley et al, 2010, Ahn et al., 2010a, 2010b, Ye et al., 2014). Although N_2O emission factors reported for full-scale systems are relatively low, from 0.01% to 1.8% of influent total nitrogen (TN) (Ahn et al., 2010a), N_2O emissions can contribute substantially to the carbon footprint of wastewater treatment plants (WWTP). It should be noted that an emission factor of 1.0% would already increase the carbon footprint of a WWTP by approximately 30% (de Haas and Hartley, 2004, Law et al., 2012). Therefore, the development of reliable predictive tools for quantifying and mitigating N_2O emission is important for achieving greenhouse gas neutral wastewater treatment (Ni et al., 2013a, 2013b).

The N_2O emission data collected from wastewater treatment plants (WWTPs) to date show a huge variation in the N_2O emission factor (the fraction of influent nitrogen load emitted as N_2O), ranging between 0.01% and 1.8%, and in some cases even higher than 10% (Kampschreur et al., 2009, Ahn et al., 2010a, 2010b, Foley et al., 2010, Wang et al., 2011). A high degree of temporal variability in N_2O emission has also been observed within the same WWTP (Ahn et al., 2010a, Ye et al., 2014). The observed variability is in clear contrast with

the fixed emission factors currently applied to estimating N_2O emissions from wastewater treatment as recommended by the United Nation's Intergovernmental Panel on Climate Change (IPCC) and various governments (IPCC, 2007, EPA, 2012). A major problem with the use of fixed emission factors is that the link between emissions and process configurations and operating characteristics is not considered. As such, the estimates do not account for the variable process conditions in different plants and do not encourage mitigation efforts (Ni et al., 2013a).

Mathematical models have been widely applied to the prediction of nitrogen removal in wastewater treatment, and are gaining more attention for the prediction of N_2O accumulation and emission during nitrification and denitrification processes (CH2MHill, 2008, Ni et al., 2011, Corominas et al., 2012, Pocquet et al., 2013, Guo and Vanrolleghem, 2014; Harper et al., 2015). The ability to predict N_2O production by modeling provides an opportunity to include N_2O production as an important consideration in the design, operation and optimization of biological nitrogen removal processes (Ni et al., 2011, 2013a). Furthermore, mathematical modelling should be a more appropriate method for estimating site-specific emissions of N_2O than the oversimplified model with fixed N_2O emission factors (Corominas et al., 2012, Ni et al., 2011, 2013a, Mampaey et al., 2013, Pocquet et al., 2013, Guo and Vanrolleghem, 2014). In addition, mathematical modeling provides a method for verifying hypotheses related to the mechanisms for N_2O production, and thus serves as a tool to support the development of mitigation strategies (Ni et al., 2013b).

N_2O modelling has evolved rapidly in the past few years, with models based on various production pathways proposed. These models have been calibrated with data obtained from laboratory reactors and full-scale wastewater treatment plants operated under various conditions. Each of these models has its underlying assumptions and has been calibrated/validated to various degrees based on the understanding of the processes of the

distinct model creators, which displayed various predictive abilities (usually good fit with own data but fail with foreign data). Despite the obvious importance of N_2O modeling, and the increasing number of publications, there has never been any attempt to summarize all the modeling information in a comprehensive review. Therefore, this review aims to clarify, to compare, and to provide guide for the use of these models. The existing mathematical models describing all the known microbial pathways for N_2O production as well as their underlying assumptions are reviewed, discussed and compared, including the single-pathway and two-pathway models of AOB, the N_2O models of heterotrophic denitrifiers, and the integrated N_2O models by both AOB and heterotrophic denitrifiers. An overview of the model evaluations using lab-scale and full-scale experimental data is also presented to provide insights into the applicability of these N_2O models under various conditions.

2. N_2O Production Pathways in Wastewater Treatment

N_2O is produced during biological nitrogen removal in wastewater treatment, typically attributed to autotrophic AOB (Tallec et al., 2006, Kampschreur et al., 2009, Chandran et al., 2011) and heterotrophic denitrifiers (Kampschreur et al., 2009, Lu and Chandran, 2010, Pan et al., 2012). Although N_2O might be potentially produced through chemical pathway (Schreiber et al., 2009; Harper et al., 2015), there are three main microbial pathways involved in N_2O formation (Figure 1), namely the NH_2OH oxidation, nitrifier (AOB) denitrification, and heterotrophic denitrification pathways (Wunderlin et al., 2012, 2013).

2.1. N_2O production by AOB

AOB are chemolithotrophs that oxidize ammonia (NH_3) to nitrite (NO_2^-) via hydroxylamine (NH_2OH) as their predominant energy-generating metabolism (Arp and Stein, 2003, Arp et al., 2007) (Figure 1A). The first step is catalyzed by ammonia monooxygenase (AMO) where NH_3 is oxidized to NH_2OH with the reduction of molecular oxygen (O_2). In

the second step, NH_2OH is oxidized to NO_2^- by hydroxylamine oxidoreductase (HAO), with O_2 as the primary electron acceptor. However, AOB contain a periplasmic copper-containing nitrite reductase (NirK) and a nitric oxide reductase (Nor) (Hooper et al., 1997, Chandran et al., 2011) (as shown in Figure 1A). NirK could speed up NH_2OH oxidation by channeling electrons from the cytochrome pool to NO_2^- (to form NO) and thus play a facilitative role in NH_3 oxidation itself (Hooper et al., 1997, Chandran et al., 2011). AOB also possess the inventory to alternatively convert NO into N_2O, using a haem–copper nitric oxide reductase, sNOR (Chandran et al., 2011).

Although N_2O is not an obligate intermediate in NH_3 oxidation, N_2O can be produced by AOB through two major pathways according to the current understanding (Figure 1A): i) N_2O as a byproduct of incomplete oxidation of NH_2OH to NO_2^-, typically referred to as the NH_2OH oxidation pathway (Poughon et al., 2000, Chandran et al., 2011, Stein, 2011a, Law et al, 2012), and ii) N_2O as the final product of AOB denitrification with NO_2^- as the terminal electron acceptor and NO as an intermediate, the so-called nitrifier or AOB denitrification pathway (Chandran et al., 2011, Ni et al., 2013b, Stein, 2011b).

It is generally accepted that NO_2^- and NO reduction for N_2O production is carried out by AOB under oxygen limiting or completely anoxic conditions (Kampschreur et al., 2009, Law et al., 2013). Increased N_2O production under high NO_2^- concentrations has been suggested to be due to AOB denitrification (Yang et al., 2009, Yu et al., 2010). On the other hand, there is also evidence supporting N_2O production from NH_2OH oxidation by AOB. The higher NH_3 oxidation rate could result in the accumulation of NH_2OH and other reaction intermediates such as NO or NOH (Law et al., 2012), which in turn result in N_2O formation with detailed reactions yet to be fully elucidated (Chandran et al., 2011, Stein, 2011a).

2.2. N_2O production by heterotrophic denitrifiers

N_2O is a known intermediate in heterotrophic denitrification (von Schulthess and Gujer,

1996, Pan et al., 2012, 2013a). Heterotrophic denitrification converts the nitrate and/or nitrite generated from autotrophic nitrification to nitrogen gas (N_2) thus removes nitrogen from wastewater. It consists of four consecutive steps, which produce three obligatory intermediates, namely NO_2^-, NO and N_2O. These steps are individually catalyzed by four different denitrification reductases, i.e., nitrate reductase (Nar), nitrite reductase (Nir), NO reductase (NOR) and N_2O reductase (N_2OR). N_2O is produced by the sequential action of the NO_3^-, NO_2^- and NO reductases (Figure 1B).

Many factors could affect the denitrification process and thus impacting N_2O emission, such as chemical oxygen demand (COD) to N ratios, the substrate and biomass types, pH levels, temperature, among others (Lu and Chandran, 2010, Pan et al., 2012, 2013a). On the other hand, the four parallel denitrification steps could also exert influence on each other through electron competition, which could result in accumulation of various intermediates including N_2O. The four denitrification steps all require electrons from carbon oxidation, and they could face competition for electrons when the electron supply rate from carbon oxidation does not meet the demand for electrons by the four steps of denitrification combined (Pan et al., 2013a).

3. Modeling of N_2O Production by AOB

As the fundamental metabolic pathways for N_2O production by AOB are now coming to light (Kampschreur et al., 2007; Schreiber et al., 2009; Yu et al., 2010; Okabe et al., 2011; Stein, 2011a; Perez-Garcia et al., 2014; Castro-Barros et al., 2015; Harris et al., 2015), several mechanistic models have been proposed for N_2O production by AOB in mixed culture based on one or two of the known N_2O production pathways of AOB, i.e., AOB denitrification and NH_2OH oxidation pathways. To date, two categories of N_2O models by AOB in mixed culture have been proposed, which are represented by single-pathway models

and two-pathway models. Tables S1 in the supplementary information (SI) lists the definitions of the all the state variables used in the two categories of models.

3.1. Single-pathway models

Six different single-pathway model structures available in literature are presented in Table S2 in SI, detailed with their kinetic and stoichiometric matrices. Table 1 presents the key differences among the model structures of these single-pathway models by AOB.

Model A (Ni et al., 2011) and Model B (Mampaey et al., 2013) are based on the AOB denitrification pathway. In Model A (Table 1, Ni et al., 2011), AOB denitrification with NO_2^- as the terminal electron acceptor produces NO and subsequently N_2O by consuming NH_2OH as the electron donor. Similarly, in Model B (Table 1, Mampaey et al., 2013), AOB denitrification occurs in parallel with ammonium oxidation, reducing NO_2^- to NO and then to N_2O with ammonium as the electron donor. The key difference between these two models is that in Model A, dissolved oxygen (DO) is assumed to inhibit nitrite and NO reduction by AOB, while in Model B, this inhibition is absent. A further minor difference is that ammonia oxidation is modelled as a two-step (ammonia to hydroxylamine and then to nitrite) process in Model A, but as a one-step process (ammonia to nitrite) in Model B.

Model A1 (Pocquet et al., 2013) and Model B1 (Guo and Vanrolleghem, 2014) are also based on AOB denitrification pathway, which are the two modified versions from Models A and B to describe N_2O production in several studies (Pocquet et al., 2013, Guo and Vanrolleghem, 2014). In Model A1 (Table 1, Pocquet et al., 2013), the oxygen inhibition of the AOB denitrification pathway was removed. In addition free ammonia (FA) and free nitrous acid (FNA) were considered as the substrate for the AOB reactions, in order to explicitly consider the effect of pH variation. In Model B1 (Table 1, Guo and Vanrolleghem, 2014), oxygen limitation and inhibition was added through a Haldane function in both the kinetics of nitrite reduction and NO reduction processes (Guo and Vanrolleghem, 2014).

Inhibition by FA was also considered in Model A1 and both inhibition by FA and FNA were included in Model B1.

Model C (Law et al., 2012) and Model D (Ni et al., 2013b) are based on the NH_2OH oxidation pathway. Model C assumes that N_2O production is due to the chemical decomposition of the unstable NOH, an intermediate of NH_2OH oxidation (Law et al., 2012). In contrast, Model D assumes that the reduction of NO, produced from the oxidation of NH_2OH, resulted in N_2O production by consuming NH_2OH as the electron donor. Model D (Table 1, Ni et al., 2013b) assumes that DO has no inhibitory effect on NO reduction (Yu et al., 2010), as in Model B.

3.2. Two-pathway models

A new approach has been employed to integrate the two N_2O production pathways of AOB into a two-pathway model, i.e., decoupling approach based on electron balance. Two different two-pathway N_2O model structures of AOB in mixed culture are presented in Table S3 in SI, detailed with their kinetic and stoichiometric matrices. Table 1 compares the key differences between these two two-pathway models by AOB.

In Model E (Table 1, Ni et al., 2014), the complex biochemical reactions and electron transfer processes involved in AOB metabolism are lumped into three oxidation and three reduction reactions (Figure 2A). Electron carriers are introduced as a new component in the model to link electron transfer from oxidation to reduction. By decoupling the oxidation (E-1 to E-3 in Figure 2A) and reduction (E-4 to E-6 in Figure 2A) reactions through the use of electron carriers, the electron distribution between O_2, NO_2^- and NO as electron sinks is modeled through assigning different kinetic values to Processes E-4, E-5 and E-6 with respect to electron carriers, which are provided by Processes E-2 and E-3. In this way, the model can predict the relative contribution of the two pathways to total N_2O production by AOB, as well as the shifts of the dominating pathway at various DO and nitrite levels conditions.

Model F (Peng et al., 2015a) is based on decoupling approach with both electron and energy (ATP) balance, which are proposed by extension of Model E to describe the dependency of N_2O production by AOB on inorganic carbon (IC) concentration (Peng et al., 2015a). In Model F (Table 1, Peng et al., 2015a), in addition to the electron carriers that link electron transfer from oxidation to reduction, Adenosine triphosphate (ATP)/Adenosine diphosphate (ADP) are also introduced as a component in the model (Table 1) to link energy generation to IC fixation for biomass growth (Figure 2B). The energy distribution between ammonia oxidation, NO_2^- reduction and oxygen reduction as energy source (ATP) is modeled through assigning different kinetic values to Processes F-1, F-5 and F-6 with respect to ADP, which are consumed by Processes F-7 with IC as substrate for AOB growth. In this way, the possible effect of IC on AOB growth and subsequently the N_2O production from different pathways by AOB can be explicitly described when the IC concentration in the bioreactor varies temporarily or spatially, with N_2O production increasing with the increase of IC levels.

4. Modeling of N_2O Production by Heterotrophic Denitrifiers

To predict denitrification intermediates accumulation, denitrification needs to be modeled as a multiple-step process (von Schulthess and Gujer, 1996). Four-step denitrification models have been proposed and widely applied to predict the accumulation of all denitrification intermediates including N_2O (Kampschreur et al., 2007, Hiatt and Grady, 2008, Ni et al., 2011, Pan et al., 2013b). To date, two distinct concepts have been proposed (Table 1), which are represented by the Activated Sludge Model for Nitrogen (ASMN) (Hiatt and Grady 2008) and the Activated Sludge Model with Indirect Coupling of Electrons (ASM-ICE) (Pan et al., 2013b), respectively. Table S4 in SI lists the kinetic and stoichiometric matrices for the two models, which are fundamentally different in describing the electron allocation among different steps of heterotrophic denitrification (Table 1).

4.1. Activated sludge model for nitrogen (ASMN)

The *"direct coupling approach"*, represented by ASMN (Model G in Table 1, Hiatt and Grady 2008), with which the carbon oxidation and nitrogen reduction processes are directly coupled in the model. This type of model describes each of the four steps as a separate and independent oxidation-reduction reaction (Table S4 in SI), with the kinetics of each step modeled according to the nitrogen reduction reaction kinetics using a stoichiometric relationship obtained through electron balance. Model G ignores the fact that the nitrogen oxides reduction and carbon oxidation are carried out by different enzymes with their specific kinetics, and consequently either of the two processes could limit the rate of denitrification. In addition, this coupling approach describes each denitrification step independently with its rate not being affected by other denitrification steps that draw electrons from the same electron supply. Essentially, the carbon oxidation rate is modeled as the sum of the carbon requirements by all denitrification steps, with the underlying assumption that electron supply will always be able to meet the predicted total electron demand.

4.2. Activated sludge model with indirect coupling of electrons (ASM-ICE)

The *"indirect coupling approach"*, proposed by Pan et al. (2013b) and named as ASM-ICE, with which the carbon oxidation and nitrogen reduction processes are decoupled. Electron carriers are introduced as a new component in this model to link carbon oxidation to nitrogen oxides reduction, with carbon oxidation reduces carriers and nitrogen oxides reduction oxidizes carriers (Model H in Table 1, Pan et al., 2013b). In this way, each step of heterotrophic denitrification can be regulated by both the nitrogen reduction and the carbon oxidation processes. The possibility of the carbon oxidation or electron transfer being a limiting step in denitrification is thus considered in the model. In heterotrophic denitrifiers, competition for electrons may occur between the four reduction steps when the electron supply rate from the oxidation process could not meet the demand for electrons by the four

reduction steps (Pan et al., 2013b), which plays an important role in the accumulation and emission of N_2O (Pan et al., 2013a). The electron competition between the four denitrifying steps can be modeled through assigning different values to the affinity constants responsible for Processes H-2, H-3, H-4 and H-5 with respect to *Mred*, which are provided by Processes H-1. Model H can be used as a practical tool for predicting N_2O accumulation during denitrification, with the complex biochemical reactions and electron transfer processes involved in biological denitrification by different microbial species being lumped into one oxidation and four reduction reactions that are linked through electron carriers.

5. Integrated N_2O Models Incorporating AOB and Heterotrophic Denitrifiers

N_2O is generally produced/consumed by both AOB and heterotrophic denitrifiers in WWTPs (Kampschreur et al., 2009, Law et al., 2012). Therefore, the integrated N_2O models incorporating N_2O production/consumption by both AOB and heterotrophic denitrifiers would contribute to more powerful models that predict the N_2O dynamics more accurately in WWTPs, which could also be useful tool for the development of N_2O mitigation strategies.

Two approaches have been reported to integrate the N_2O production/consumption by both AOB and heterotrophic denitrifiers into a comprehensive N_2O model: i) ASM-type models that combine one of the single-pathway models of AOB (e.g., Models A-D, Table S2) with ASMN of heterotrophic denitrifiers (Model G, Table S4) (Ni et al., 2011, Pocquet et al., 2013, Guo and Vanrolleghem, 2014, Spérandio et al., 2014), and ii) Electron balance based model that integrate the electron carrier based two-pathway model of AOB (Model E, Table S3) and ASMN (Model G, Table S4) (Ni et al., 2015). Both modeling approaches have been successfully applied to describe N_2O emissions from mixed culture nitrification-denitrification systems and to identify the relative contributions between AOB and heterotrophic denitrifiers to total N_2O production (Ni et al., 2011, 2013b, 2015,

Spérandio et al., 2014). A third potential approach to integrate the N_2O production/consumption by both AOB and heterotrophic denitrifiers could be a full electron balance based model integrating the electron carrier based two-pathway model of AOB (Model E, Table S3) and electron carrier based model of heterotrophs (Model H, Table S4), which though require future testing. It should be noted that the possible consumption of N_2O by heterotrophic denitrification as a N_2O sink may occur and reduce overall N_2O production in integrated model under the conditions of high COD to N ratio and/or low DO level.

6. Model Calibration, Validation and Selection

The N_2O models have to be tested to predict N_2O emission data from experiments in order for the models to be developed into a useful tool for practical applications. During past years, measurement campaigns have been performed by many studies. All the available N_2O models have been evaluated with experimental data collected from different systems to reveal the performance of these models under various process conditions and shed light on the conditions under which each of the models would be suitable to facilitate their applications.

6.1. Model Evaluation against Experimental Data

The six single-pathway models of AOB (Models A-D, Table 1) was evaluated and compared (Ni et al., 2011; Ni et al., 2013a; Spérandio et al., 2014) based on their ability to capture the observed N_2O production results from different experiments (Yang et al., 2009; Kim et al., 2010; Law et al., 2012; Spérandio et al., 2014). Model A could well predict the observed trend of decrease in N_2O production at high DO concentrations (Yang et al., 2009), whereas Model B was not able to predict such trend due to the absence of oxygen inhibition on AOB denitrification in Model B (Ni et al., 2013a). Model B could not describe well the N_2O peak that is likely related to the dynamics of NH_2OH (Ni et al., 2013a), which was not included in Models B and B1. Models A, A1, B and B1 have been tested to be able to

reasonably describe N_2O production data with high nitrite accumulation (Spérandio et al., 2014). In contrast, both Models C and D were not able to capture the observed dependency of N_2O production on nitrite availability (Yang et al., 2009, Kim et al., 2010, Spérandio et al., 2014) due to the fact that the two models are linked to incomplete NH_2OH oxidation. However, Models C and D were able to reproduce the experimental observations that the N_2O production increased/decreased with increasing/decreasing DO concentration (Law et al., 2012). The kinetic structure of Model B also ensured that the N_2O production rate is dependent on oxygen availability, resulting in a similar N_2O dynamic trend (increase in the N_2O production rate with a increase in DO concentration). On the contrary, Model A predicted an opposite to such observation (Law et al., 2012). These results suggested that DO inhibition might be required to describe AOB denitrification pathway and NH_2OH need to be included as a necessary intermediate. The use of FA and FNA in model structures would be recommend for a better description of the pH effect and possible FNA inhibition. NOH would be preferably used as N_2O precursor for describing NH_2OH pathway under extremely high nitrite accumulation condition whereas NO could be generally applied as intermediate for N_2O production from NH_2OH oxidation under common wastewater conditions.

With respect to the two-pathway models of AOB, Model E has satisfactorily described the N_2O data from several different nitrifying cultures (partial nitritation culture or/and full nitrification culture) and under various DO and NO_2^- concentration conditions (Ni et al., 2014, Peng et al., 2014; Sabba et al., 2015). Model F has also well predicted these different nitrifying cultures (partial nitritation and full nitrification culture) and under various IC conditions (Peng et al., 2015a). These two-pathway models also successfully predicted shifts of the dominating pathway at various DO, nitrite and/or IC levels (see Figure 3), consistent with experimental observations that N_2O was produced from both nitrifier denitrification and NH_2OH oxidation pathways by AOB (Ni et al., 2014; Peng et al., 2014). The model results

suggested that the contribution of AOB denitrification decreased as DO increased, accompanied by a corresponding increase in the contribution by the NH_2OH oxidation pathway, which were verified by the site preference (SP) isotopic measurements (Peng et al., 2014). Although the electron based two-pathway models (Models E and F) have been demonstrated to be effective, electron carriers may not necessarily be the only approach to the integration of the two pathways into one model. The possible alternatives/simplifications could be evaluated in the future.

For denitrifying N_2O models, Model G was generally able to reproduce the nitrate, nitrite and N_2O profiles when only one nitrogen oxide species was added (Ni et al., 2011, Pan et al., 2015), but Model G failed to reproduce the results when two or more nitrogen oxide species were added together. In contrast, Model H was shown to be able to describe general COD consumption, nitrate reduction and nitrite accumulation by enriched denitrifying culture (Pan et al., 2015), the influence of nitrite and N_2O addition on nitrate reduction, as well as the experimental results when one or more nitrogen oxide species were added (Pan et al., 2015). Therefore, the decoupling approach of Model H (Table 1) might be essential to describe the electron competition process among the four denitrifying steps.

6.2. Selection of Models for N_2O Prediction

The model evaluation results strongly suggest that appropriate selection of available N_2O models is important for accurate N_2O prediction in different engineering nitrogen removal systems under different operational conditions. Table 2 present a possible guideline for model selection in their further applications.

For N_2O production by AOB, the single-pathway models (Models A-D) have simplifier structures (one single pathway involved) and fewer parameters, which bring convenience to model calibration (Table 2), and could be used preferentially under certain conditions, although they are not be able to reproduce all the N_2O data. The two-pathway models (Models

E-F) have the potential to describe all the N_2O data with different operational conditions, but may require more efforts on model calibration because of more parameters. Specifically (Table 2), Models A, A1, B and B1 might be used to describe the regulation of N_2O production by nitrite (or FNA) concentration. Models C and D might be able to describe N_2O emissions from the systems with the condition of relatively high DO levels and low nitrite accumulation that likely favoring the NH_2OH oxidation pathway for N_2O production. In addition, according to the analysis by Peng et al. (2015b) (Figure 4), it is critical that the DO concentration in the system is well controlled at a constant level for the AOB denitrification model to be used (e.g., Model A). The NH_2OH oxidation model (e.g., Model D) can be applied under high DO conditions. Under other conditions, the two-pathway models (e.g., Model E) should be applied. Model E could be used under varying DO and NO_2^- but constant IC conditions while Model F should be applied under highly dynamic IC condition.

For N_2O production by heterotrophic denitrifiers, Model G can be used to predict the overall nitrogen and COD removal performance in a wastewater treatment plant as in most cases the low level accumulation of denitrification intermediates do not significantly affect the overall nitrogen removal rate. However, in the context of predicting the N_2O production by heterotrophic denitrifiers, Model G is inadequate due to its structurally deficient in describing the electron competition process in denitrification. Model H enhanced our ability to predict N_2O production by heterotrophic denitrifiers and has the potential to describe all the N_2O data under different conditions, but requires information on both the carbon oxidation reaction kinetics and the nitrogen reduction kinetics.

6.3. Key Kinetic and Stoichiometric Parameters

Table S5 in SI summarizes the typical values of the model parameters that have been reported in literature, which could serve as default values for the future applications of the available N_2O models (Tables S2-S4). The continued testing against more experimental data

would delineate a range/pattern in parameter values. It should be noted that these parameters were estimated under different conditions of temperature, sludge retention time and feeding composition, and therefore correction factors must be adjusted by, for example, Arrhenius equations (Snip et al., 2014). Furthermore, the parameter values estimated during batch experiments may not be adequate for the continuous process and may not be compatible with the values of other parameters (Ni et al., 2013a, Spérandio et al., 2014, Snip et al., 2014).

For the six single-pathway models of AOB (Models A-D in Table S2), the model parameters were obtained after significant calibration efforts, and thus some of the parameters showed high variation (more than 100%) among case studies during model evaluations (Ni et al., 2011, Ni et al., 2013a, Spérandio et al., 2014). Among them, the half saturation constant for nitrite or FNA ($K_{NO2,AOB}$ or $K_{HNO2,AOB}$ for Models A, A1, B, B1) and the reduction factor for N_2O production (η_{AOB}, for all the six single-pathway models) were most highly variable (see Table S5 in SI) and very influential on N_2O emissions (Spérandio et al., 2014). Regarding the models based on AOB denitrification pathway (e.g., Models A, A1, B and B1) the large variation of these two key parameters were related to the range of nitrite (or FNA) concentration observed in each system (Spérandio et al., 2014), likely due to the adaptation of enzymatic activity (NirK). Regarding the models based on NH_2OH oxidation pathway (e.g., Models C and D) the large variation of η_{AOB} might be dependent on the possible NO accumulation in each system. High NO accumulation would lead to a low value for η_{AOB} (Spérandio et al., 2014). Thus, calibration will be required for the application of the single-pathway models regarding these key parameters (Table 2).

For the electron balance based two-pathway models of AOB (Models E and F in Table S3), the affinity constants with respect to electrons (e.g., $K_{Mred,3}$, and $K_{Mred,4}$) are unique to the two-pathway models and the key parameters governing the N_2O production via the two pathways. The values represent the affinity of the corresponding reduction reaction to

electrons, with lower values indicating a higher affinity and thus a higher ability to compete for electrons. For example, the estimated $K_{Mred,3}$ has a value that is about one magnitude smaller than $K_{Mred,4}$ (Ni et al., 2014), indicating that O_2 reduction has a higher ability to compete for electrons as the main electron acceptor during NH_2OH oxidation. Ni et al. (2014) revealed that the absolute value of C_{tot} is not critical for model calibration and predictions, and it is the ratios between parameters K_{Mox}, $K_{Mred,1}$, $K_{Mred,2}$, $K_{Mred,3}$, and $K_{Mred,4}$ and parameter C_{tot} that affect the model output. Therefore, attention should be paid to these ratios for the calibration and application of the two-pathway models (see Table 2).

Regarding the ASM-ICE of heterotrophic denitrifiers (Model H in Table S4), information on both the carbon oxidation reaction kinetics and the nitrogen reduction kinetics was required for its calibration and application (Table 2). Due to the lack of understanding of the electron competition process in most of the previous studies, the respective reaction kinetics of the carbon oxidation and nitrogen reduction processes were not well established. For instance, the maximum carbon source oxidation rate ($r_{COD,\max}$), which is the key parameter to restrict the overall model predicted carbon oxidation (electron supply) rate, is not available in literature and thus need to be measured or estimated (Pan et al., 2015). Similar to the two-pathway models of AOB, the relative ratios between electron affinity constants ($K_{Mred,1}$, $K_{Mred,2}$, $K_{Mred,3}$, and $K_{Mred,4}$) rather than their absolute values are important for the reaction rate. Therefore, more efforts are needed to provide more information on these key parameters of the ASM-ICE model for its further implementation (Table 2).

7. Application of N_2O Models in Full-Scale WWTPs

Mathematical modelling of N_2O emissions from full-scale WWTPs was firstly conducted successfully by using ASM-type models that combine one of the single-pathway models of AOB with ASMN of heterotrophic denitrifiers (Ni et al., 2013b). Ni et al. (2013b) applied a

model based on NH_2OH pathway model of AOB (Model D, Table 1) and ASMN (Model G, Table 1) to describe the N_2O emissions from full-scale WWTPs. The model described well the dynamic ammonium, nitrite, nitrate, DO and N_2O data collected from both an open oxidation ditch (OD) system with surface aerators and a SBR system with bubbling aeration. Ni et al. (2013b) also performed additional evaluations on the other three single-pathway N_2O models of AOB (Model A, Model B and Model C in Table 1) to evaluate the experimentally observed N_2O data from the two full-scale WWTPs. The results indicated that Model A could not predict the N_2O data from either WWTP (Ni et al., 2013b, Spérandio et al., 2014). Models B and C, on the contrary, obtained very similar fit between the model-predicted and experimentally observed N_2O data (Ni et al., 2013b, Spérandio et al., 2014).

Dynamic simulations were also confronted to the data collected on the UCT process from Eindhoven plant by using ASM-type models that combine one of the single-pathway models of AOB with ASMN of heterotrophic denitrifiers (Guo and Vanrolleghem, 2014; Spérandio et al., 2014). Model A1 + Model G, Model B1 + Model G and Model D + Model G were all implemented for this plant and calibrated using date collected in a 1-month measurement campaign. The conclusion was that all these models could be calibrated to the same level of fit (Spérandio et al., 2014). They had similar performance and could follow the dynamic variations in the measured N_2O data (see Figure 5). In addition, results showed that there was less N_2O emission under wet-weather conditions compared to dry-weather conditions and all the three models showed better simulation performance under dry-weather conditions than wet-weather conditions (Spérandio et al., 2014).

Mathematical modelling of N_2O emissions from full-scale WWTPs was then conducted successfully by using electron balance based model that integrate the two-pathway model of AOB and ASMN of heterotrophic denitrifiers (Ni et al., 2015). Ni et al. (2015) applied an integrated model incorporating the electron balance based two-pathway model of AOB

(Model E, Table 1) and ASMN of heterotrophic denitrifiers (Model G, Table 1) to describe N_2O emissions from a step-feed full-scale WWTP. The model described well all the dynamic ammonium, nitrite, nitrate, DO and N_2O emission data. Modeling results revealed that the AOB denitrification pathway decreased and the NH_2OH oxidation pathway increased along the path of the both Steps, with the Second Step of the full-scale WWTP having much higher N_2O emission than the First Step. The integrated N_2O model captured all these trends regarding the shifting/distribution between the different N_2O pathways in full-scale WWTP (see Figure 6). A potential strategy to mitigate N_2O emission from this plant is also evaluated using the model. The overall N_2O emission from the step-feed WWTP would be largely mitigated if 30% of the returned activated sludge was returned to the Second Step with the remained 70% returning to the First Step. The model could potentially serve as a powerful tool for the prediction of N_2O emissions from full-scale WWTPs and development of effective mitigation strategies, although it may require more efforts on model calibration.

It should be noted that there are still limited number of studies presented in literature regarding the real application of N_2O models in full-scale WWTPs although many full-scale measurement campaigns have been performed in different places during the past years. More full-scale applications of the models using these full-scale N_2O data are still needed for the models to be developed into a useful tool for practical applications. In addition, the requirement of good fundamental knowledge on N_2O emission from modeller/engineer might also hinder the N_2O model applications due to the complicated procedure for model selection and calibration, which consequently limit the development of effective mitigation strategies. Hopefully this review would facilitate the selection of suitable N_2O models, the estimation of site-specific N_2O emissions and the development of mitigation strategies for a wastewater treatment plant taking into the specific design and operational conditions of the plant.

8. Conclusions and Perspectives

In this work, the existing N_2O models available in literature based on the three major N_2O production pathways were reviewed and compared to illuminate their structural differences, their capabilities and inabilities describing experimental data and their potential range of applications. The key conclusions are:

- The fundamental mechanism about N_2O production is still not fully understood, leading to the structural differences of existing N_2O models and their capabilities/inabilities describing experimental data under different conditions.
- For AOB, the two-pathway models have the potential to describe all the N_2O data, but may require more efforts on model calibration. The single-pathway models could be used under several particular conditions. For heterotrophic denitrifiers, the ASMN-type model is preferred for predicting the overall nitrogen and COD removal performance with low intermediates accumulation. The ASM-ICE type model has the potential to describe all the N_2O data, but requires more information on reaction kinetics.
- The available lab- and full-scale data sets are not well consolidated with highly different reactor set-ups, measurement methods, culture history, documentations, and/or interpretations, which would possibly lead to the failure of model predictions.
- Although the good fundamental knowledge on N_2O emission from modeller is essential for successful application, mathematical modeling of N_2O production has reached a maturity that facilitates the estimation of site-specific N_2O emissions and the development of mitigation strategies.

Although existing models still have limitations, their application will undoubtedly increase in the near future. Work in the following areas is necessary in order to gain a better modeling of N_2O emission:

- While the electron balance based model has been successfully applied to estimate

site-specific N_2O emissions and develop mitigation strategies for a specific WWTP, future efforts should be devoted to comparing the selected models to real data from real WWTPs to observe the key differences and to enhance their practical applications.

- The parameters obtained with different experiments and cultures should be compared and synthetized, aiming to form a consistent pattern which could then be implemented in the improvement/simplification of multiple-pathway model, and integrated with the models describing other sections of the WWTPs to from a powerful plant wide model.
- Mathematical modeling of N_2O emission from biofilm systems should be conducted using more monitoring data from such systems.
- The real application of N_2O models in full-scale WWTPs using more full-scale measurement campaigns would still be required for the models to be developed into a useful tool for practical applications. Model-based development of mitigation strategies should be further conducted, with their validities being tested in real operations.

Acknowledgements

Dr. Bing-Jie Ni acknowledges the supports of Australian Research Council (ARC) Discovery Early Career Researcher Award DE130100451 and ARC Discovery Project DP130103147.

References

Ahn, J. H., Kim, S., Park, H., Rahm, B., Pagilla, K., Chandran, K. 2010a. N_2O emissions from activated sludge processes, 2008−2009: results of a national monitoring survey in the United States. Environ. Sci. Technol. 44, 4505-4511.

Ahn, J. H., Kim, S., Park, H., Katehis, D., Pagilla, K., Chandran, K. 2010b. Spatial and temporal variability in atmospheric nitrous oxide generation and emission from full-scale

526 biological nitrogen removal and non-BNR processes Water Environ. Res. 82, 2362-2372.
527 Arp, D. J., Chain, P. S. G., Klotz, M. G. 2007. The impact of genome analyses on our
528 understanding of ammonia-oxidizing bacteria. Annu. Rev. Microbiol. 61, 503-528.
529 Arp, D. J., Stein, L. Y. 2003. Metabolism of inorganic N compounds by ammonia-oxidizing
530 bacteria. Crit. Rev. Biochem. Mol. Biol. 38, 471-495.
531 Castro-Barros, C. M., Daelman, M. R. J., Mampaey, K. E., van Loosdrecht, M. C. M., Volcke
532 E. I. P. 2015. Effect of aeration regime on N_2O emission from partial
533 nitritation-anammox in a full-scale granular sludge reactor. Water Res. 68, 793-803.
534 Chandran, K., Stein, L. Y., Klotz, M. G., van Loosdrecht, M. C. M. 2011. Nitrous oxide
535 production by lithotrophic ammonia-oxidizing bacteria and implications for engineered
536 nitrogen-removal systems. Biochem. Soc. Trans. 39, 1832-1837.
537 Corominas, L., Flores-Alsina, X., Snip, L., Vanrolleghem, P.A. 2012. Comparison of different
538 modelling approaches to better understand and minimize greenhouse gas emissions from
539 wastewater treatment plants. Biotechnol. Bioeng. 109, 2854-2863.
540 CH2MHill. 2008. Discussion paper for a wastewater treatment plant sector greenhouse gas
541 emissions reporting protocol, Final report prepared for California Wastewater Climate
542 Change Group, Oakland, California.
543 de Haas, D., Hartley, K. J. 2004. Greenhouse gas emissions from BNR plant – do we have the
544 right focus? Proceedings: Sewage Management – Risk Assessment and Triple Bottom
545 Line. Queensland Environmental Protection Agency, Cairns (April 2004), pp. 5-7.
546 Foley, J., de Haas, D., Yuan, Z., Lant, P. 2010. Nitrous oxide generation in full-scale
547 biological nutrient removal wastewater treatment plants. Water Res. 44, 831-844.
548 Guo, L., Vanrolleghem, P. A. 2014. Calibration and validation of an Activated Sludge Model
549 for Greenhouse gases No. 1 (ASMG1) - Prediction of temperature dependent N_2O
550 emission dynamics. Bioprocess Biosyst. Eng. 37, 151-163.

ACCEPTED MANUSCRIPT

551 Harper, Jr. W. F., Takeuchi, Y., Riya, S., Hosomi, M., Terada, A. 2015. Novel abiotic reactions
552 increase nitrous oxide production during partial nitrification: Modeling and experiments.
553 Chem. Eng. J. 281, 1017-1023.
554 Harris, E., Joss, A., Emmenegger, L., Kipf, M., Wolf, B., Mohn, J., Wunderlin, P. 2015.
555 Isotopic evidence for nitrous oxide production pathways in a partial nitritation-anammox
556 reactor. Water Res. 83, 258-270.
557 Hiatt, W. C., Grady, Jr. C. P. L. 2008. An updated process model for carbon oxidation,
558 nitrification, and denitrification. Water Environ. Res. 80, 2145-2156.
559 Hooper, A. B., Vannelli, T., Bergmann, D. J., Arciero, D. M. 1997. Enzymology of the
560 oxidation of ammonia to nitrite by bacteria. Antonie van Leeuwenhoek 71, 59-67.
561 Inventory of U.S. Greenhouse Gas Emissions and Sinks: 1990-2010, EPA 430-R-12-001, U.
562 S. Environmental Protection Agency: Washington, DC, 2012.
563 IPCC (2007) Climate Change 2007: The Physical Science Basis. Contribution of Working
564 Group I to the Fourth Assessment Report of the Intergovernmental Panel on Climate
565 Change [Solomon, S., D. Qin, M. Manning, Z. Chen, M. Marquis, K.B. Averyt, M.Tignor
566 and H.L. Miller (eds.)]. Cambridge University Press, Cambridge, United Kingdom and
567 New York, NY, USA.
568 Kampschreur, M. J., Picioreanu, C., Tan, N., Kleerebezem, R., Jetten, M. S. M., van
569 Loosdrecht, M. C. M. 2007. Unraveling the source of nitric oxide emission during
570 nitrification. Water Environ. Res. 79, 2499-2509.
571 Kampschreur, M. J., Temmink, H., Kleerebezem, R., Jetten, M. S. M., van Loosdrecht, M. C.
572 M. 2009. Nitrous oxide emission during wastewater treatment. Water Res. 43,
573 4093-4103.
574 Kim, S. W., Miyahara, M., Fushinobu, S., Wakagi, T., Shoun, H. 2010. Nitrous oxide
575 emission from nitrifying activated sludge dependent on denitrification by

ammonia-oxidizing bacteria. Bioresour. Technol. 101, 3958-3963.

Law, Y., Ni, B. J., Lant, P., Yuan, Z. 2012. Nitrous oxide (N_2O) production by an enriched culture of ammonia oxidising bacteria depends on its ammonia oxidation rate. Water Res. 46, 3409-3419.

Law, Y., Lant, P. A., Yuan, Z. 2013. The confounding effect of nitrite on N_2O production by an enriched ammonia-oxidising culture, Environ. Sci. Technol. 47, 7186-7194.

Lu, H., Chandran, K. 2010. Factors promoting emissions of nitrous oxide and nitric oxide from denitrifying sequencing batch reactors operated with methanol and ethanol as electron donors. Biotechnol. Bioeng. 106, 390-398.

Mampaey, K. E., Beuckels, B., Kampschreur, M. J., Kleerebezem, R., Van Loosdrecht, M. C. M., Volcke, E. I. P. 2013. Modelling nitrous and nitric oxide emissions by autotrophic ammonia-oxidizing bacteria. Environ. Technol. 34, 1555-1566.

Ni, B. J., Ruscalleda, M., Pellicer-Nacher, C., Smets, B. F. 2011. Modeling nitrous oxide production during biological nitrogen removal via nitrification and denitrification: extensions to the general ASM models. Environ. Sci. Technol. 45, 7768-7776.

Ni, B.J., Yuan, Z., Chandran, K., Vanrolleghem, P.A., Murthy, S., 2013a. Evaluating four mathematical models for nitrous oxide production by autotrophic ammonia-oxidizing bacteria. Biotechnol. Bioeng. 110, 153-163.

Ni, B. J., Ye, L., Law, Y., Byers, C., Yuan, Z., 2013b. Mathematical modeling of nitrous oxide (N_2O) emissions from full-scale wastewater treatment plants. Environ. Sci. Technol. 47, 7795-7803.

Ni, B. J., Peng, L., Law, Y., Guo, J., Yuan, Z. 2014. Modeling of nitrous oxide production by autotrophic ammonia-oxidizing bacteria with multiple production pathways. Environ. Sci. Technol. 48, 3916-392.

Ni, B. J., Pan, Y., van den Akker, B., Ye, L., Yuan, Z. 2015. Full-scale modeling explaining

large spatial variations of nitrous oxide fluxes in a step-feed plug-flow wastewater treatment reactor. Environ. Sci. Technol. 49, 9176-9184.

Okabe, S., Oshiki, M., Takahashi, Y., Satoh, H. 2011. N_2O emission from a partial nitrification–anammox process and identification of a key biological process of N_2O emission from anammox granules. Water Res. 45, 6461-6470.

Pan, Y., Ye, L., Ni, B. J., Yuan, Z. 2012. Effect of pH on N_2O reduction and accumulation during denitrification by methanol utilizing denitrifiers. Water Res. 46 (15), 4832-4840.

Pan, Y., Ni, B. J., Bond, P. L., Ye, L., Yuan, Z. 2013a. Electron competition among nitrogen oxides reduction during methanol-utilizing denitrification in wastewater treatment. Water Res. 47 (10), 3273-3281.

Pan, Y., Ni, B.J., Yuan, Z. 2013b. Modeling electron competition among nitrogen oxides reduction and N_2O accumulation in denitrification. Environ. Sci. Technol. 47, 11083-11091.

Pan, Y., Ni, B.J., Lu, H., Chandran, K., Richardson, D., Yuan, Z. 2015. Evaluating two concepts for the modelling of intermediates accumulation during biological denitrification in wastewater treatment. Water Res. 71, 21-31.

Peng, L., Ni, B.J., Erler, D., Ye, L., Yuan, Z. 2014. The effect of dissolved oxygen on N_2O production by ammonia-oxidizing bacteria in an enriched nitrifying sludge. Water Res. 66, 12-21.

Peng, L., Ni, B.J., Law, Y., Yuan, Z. 2015a. Modeling of N_2O production by ammonia oxidizing bacteria: Integration of catabolism and anabolism. The 9th IWA Symposium on Systems Analysis and Integrated Assessment (Watermatex 2015), Gold Coast, Australia, June 14-17.

Peng, L., Ni, B. J., Ye, L., Yuan, Z. 2015b. Selection of mathematical models for N_2O production by ammonia oxidizing bacteria under varying dissolved oxygen and nitrite

626 concentrations. Chem. Eng. J. 281, 661-668.

627 Perez-Garcia, O., Villas-Boas, S. G., Swift, S., Chandran, K., Singhal, N. 2014. Clarifying the
628 regulation of NO/N_2O production in *Nitrosomonas europaea* during anoxic-oxic
629 transition via flux balance analysis of a metabolic network model. Water Res. 60,
630 267-277.

631 Pocquet, M., Queinnec, I., Spérandio, M. 2013. Adaptation and identification of models for
632 nitrous oxide (N_2O) production by autotrophic nitrite reduction. In: Proceedings 11th
633 IWA Conference on Instrumentation, Control and Automation (ICA2013). Narbonne,
634 France, September 18-20.

635 Portmann, R. W., Daniel, J. S., Ravishankara, A. R. 2012. Stratospheric ozone depletion due
636 to nitrous oxide: influences of other gases. Phil. Trans. R. Soc. B. 367, 1256-1264.

637 Poughon, L., Dussap, C. G., Gros, J. B. 2000. Energy model and metabolic flux analysis for
638 autotrophic nitrifiers. Biotechnol. Bioeng. 72, 416-433.

639 Sabba, F., Picioreanu, C., Pérez, J., Nerenberg, R. 2015. Hydroxylamine diffusion can
640 enhance N_2O emissions in nitrifying biofilms: a modeling study. Environ. Sci. Technol.
641 49, 1486-1494.

642 Schreiber, F., Loeffler, B., Polerecky, L., Kuypers, M. M. M., de Beer, D. 2009. Mechanisms
643 of transient nitric oxide and nitrous oxide production in a complex biofilm. ISME J. 3,
644 1301-1313.

645 Snip, L.J.P., Boiocchi, R., Flores-Alsina, X., Jeppsson, U., Gernaey, K.V. 2014. Challenges
646 encountered when expanding activated sludge models: a case study based on N_2O
647 production. Water Sci. Technol. 70(7), 1251-1260.

648 Spérandio, M., Pocquet, M., Guo, L., Vanrolleghem, P., Ni, B.J., Yuan, Z. 2014. Calibration
649 of nitrous oxide production models with continuous long-term process data. The 4th
650 IWA/WEF Wastewater Treatment Modelling Seminar (WWTmod2014), Spa, Belgium.

651 Stein, L. Y. 2011a. Surveying N_2O-producing pathways in bacteria. Methods in Enzymology
652 486, 131-152.
653 Stein, L. Y. 2011b. Heterotrophic nitrification and nitrifier denitrification. In *Nitrification*,
654 Ward, B. B., Arp, D. J., Klotz, M. G., Eds. American Society for Microbiology Press:
655 Washington D.C., pp 95-114.
656 Tallec, G., Garnier, J., Billen, G., Gousailles, M. 2006. Nitrous oxide emissions from
657 secondary activated sludge in nitrifying conditions of urban wastewater treatment plants:
658 Effect of oxygenation level. Water Res. 40, 2972-2980.
659 von Schulthess, R., Gujer, W. 1996. Release of nitrous oxide (N_2O) from denitrifying
660 activated sludge: Verification and application of a mathematical model. Water Res. 30 (3),
661 521-530.
662 Wang, J. S., Hamburg, S. P., Pryor, D. E., Chandran, K., Daigger, G. T. 2011. Emissions
663 credits: opportunity to promote integrated nitrogen management in the wastewater sector.
664 Environ. Sci. Technol. 45, 6239-6246.
665 Wunderlin, P., Lehmann, M.F., Siegrist, H., Tuzson, B., Joss, A., Emmenegger, L., Mohn, J.
666 2013. Isotope signatures of N_2O in a mixed microbial population system: constraints on
667 N2O producing pathways in wastewater treatment. Environ. Sci. Technol. 47, 1339-1348.
668 Wunderlin, P., Mohn, J., Joss, A., Emmenegger, L., Siegrist, H. 2012. Mechanisms of N_2O
669 production in biological wastewater treatment under nitrifying and denitrifying
670 conditions. Water Res. 46, 1027-1037.
671 Yang, Q., Liu, X., Peng, C., Wang, S., Sun, H., Peng, Y. 2009. N_2O Production during
672 nitrogen removal via nitrite from domestic wastewater: Main sources and control method.
673 Environ. Sci. Technol. 43, 9400-9406.
674 Ye, L., Ni, B.-J., Law, Y., Byers, C., Yuan, Z., 2014. A novel methodology to quantify nitrous
675 oxide emissions from full-scale wastewater treatment systems with surface aerators.

ACCEPTED MANUSCRIPT

676 Water Res. 48, 257–268.

677 Yu, R., Kampschreur, M. J., van Loosdrecht, M. C. M., Chandran, K. 2010. Mechanisms and
678 specific directionality of autotrophic nitrous oxide and nitric oxide generation during
679 transient anoxia. Environ. Sci. Technol. 44, 1313-1319.

ACCEPTED MANUSCRIPT

ACCEPTED MANUSCRIPT

Table 1. Key differences among the single-pathway models by AOB, two-pathway models by AOB and N_2O models by heterotrophs

N_2O models		Model components	Stoichiometric	Kinetic
Single-pathway models by AOB	Model A - AOB denitrification	Using S_{NH4} and S_{NO2}; With S_{NH2OH}.	Two-step NH_4^+ oxidation; Two-step NO_2^- reduction; Cell growth during NH_2OH oxidation.	Two different oxygen affinity constants; Oxygen inhibition on NO_2^- and NO reductions; Anoxic reduction factor.
	Model A1- AOB denitrification	Using S_{NH3} and S_{HNO2}; With S_{NH2OH}.	Same as Model A.	Two different oxygen affinity constants; Without oxygen inhibition; NH_3 inhibition on NH_3 oxidation; Anoxic reduction factor.
	Model B - AOB denitrification	Using S_{NH3} and S_{HNO2}; Without S_{NH2OH}.	One-step NH_4^+ oxidation; Two-step NO_2^- reduction; Cell growth during all 3 processes.	Only one oxygen affinity constant; Without oxygen inhibition; Anoxic reduction factor.
	Model B1 - AOB denitrification	Same as Model B.	Same as Model B.	Only one oxygen affinity constant; NH_3 and HNO_2 inhibitions on NH_3 oxidation; Haldane function for oxygen limitation; Anoxic reduction factor.
	Model C - NH_2OH pathway (via NOH)	Using S_{NH4} and S_{NO2}; With S_{NOH}.	Three-step NH_4^+ oxidation via NOH; Cell growth during NH_2OH oxidation.	Two different oxygen affinity constants; NOH breakdown to produce N_2O.
	Model D - NH_2OH pathway (via NO)	Using S_{NH4} and S_{NO2}; With S_{NO}.	Three-step NH_4^+ oxidation via NO; Cell growth during NH_2OH oxidation.	Two different oxygen affinity constants; NO reduction to produce N_2O; Without oxygen inhibition.
Two-pathway models by AOB	Model E	Using S_{NH3} and S_{NO2}; With electron carriers.	Three-step NH_3 oxidation; One-step NO_2^- reduction; Without cell growth.	Applying electron competition concept; Without oxygen inhibition; Without anoxic reduction factor.
	Model F	Mostly same as Model E; With S_{CO2}; With energy carriers.	Mostly same as Model E; With energy carriers involved; With cell growth considered.	Mostly same as Model E; With energy carriers involved; With effect of inorganic carbon considered.
N_2O models by heterotrophs	Model G	Without electron carriers.	Coupling carbon oxidation and nitrogen reduction (4 processes).	Without electron competition concept.
	Model H	With electron carriers.	Decoupling carbon oxidation and nitrogen reduction (5 processes).	With electron competition concept.

ACCEPTED MANUSCRIPT

Table 2. Guideline for model selection for predicting N_2O production by AOB and heterotrophic denitrification

N_2O models	Single-pathway models by AOB	Two-pathway models by AOB	N_2O models by heterotrophs
Applicable conditions	✓ Models A, A1, B and B1 to describe the regulation of N_2O production by nitrite (or FNA) ✓ Model A to predict possible DO inhibition on N_2O production at high DO levels ✓ Models A1, B and B1 to predict possible pH effect and FA/FNA inhibition on N_2O production ✓ Models C and D to describe N_2O emissions at high DO levels and low nitrite accumulation	✓ Model E to predict N_2O production at varying DO and NO_2^- with constant IC ✓ Model F to describe N_2O production under highly dynamic IC condition	✓ Model G to predict the overall nitrogen and COD removal performance with low level accumulation of denitrification intermediates ✓ Model H to describe N_2O production under different conditions
Inabilities of the models	✓ Model A not to describe the increase of N_2O production with increasing DO ✓ Models B and B1 not to predict the N_2O production related to the dynamics of NH_2OH ✓ Models C and D not to predict the effect of nitrite accumulation on N_2O production	✓ Model E not to describe N_2O production with dynamic IC	✓ Model G not to describe N_2O production with electron competition
Key parameters for calibration	✓ The half saturation constant for nitrite or FNA ($K_{NO2,AOB}$ or $K_{HNO2,AOB}$ for Models A, A1, B, B1) ✓ The reduction factor for N_2O production (η_{AOB}, for all the six single-pathway models)	✓ The affinity constants with respect to electrons (e.g., $K_{Mred,3}$, and $K_{Mred,4}$) ✓ The ratios among the affinity constants to electrons	✓ The N_2O production and reduction rates ✓ The relative ratios between electron affinity constants

ACCEPTED MANUSCRIPT

ACCEPTED MANUSCRIPT

Figure Legends

Figure 1. Simplified representation of the three N_2O production pathways by ammonia oxidizing bacteria (A) and heterotrophic denitrifiers (B): nitrifier denitrification, NH_2OH oxidation and heterotrophic denitrification pathways.

Figure 2. Simplified representation of the electron transfer and energy transform processes in the biochemical reactions (reaction numbers refer to Table S3 in SI) associated with N_2O production by AOB via the two production pathways: (A) Electron balance (Ni et al., 2014), and (B) Energy balance (Peng et al., 2015a).

Figure 3. The predicted contributions from the nitrifier dinitrification pathway and the NH_2OH pathway as well as their shifts using Model E (real data: symbols, model predictions: lines) for a partial nitrification (left panel adapted from Ni et al., 2014) and a full nitrification system (right panel adapted from Peng et al., 2014).

Figure 4. Summary of applicable regions for the AOB denitrification model, the NH_2OH oxidation model and the two-pathway model under various DO and NO_2^- concentrations. The applicable regions were insensitive to the variations of key parameters governing N_2O production by the two-pathway model (Peng et al., 2015b).

Figure 5. Model evaluation results for N_2O emissions using the measurement results at the beginning (BM) (upper panel), the middle (MM) (middle panel) and the end section (EM) (bottom panel) of the summer aeration package on the UCT process from Eindhoven plant by using ASM-type models that combine one of the single-pathway models of AOB (Models A1, B1 and C) with ASMN (Model G) of heterotrophic denitrifiers (Spérandio et al., 2014).

Figure 6. Model predicted percentage contributions from the three N_2O pathways to total N_2O productions at six different locations of the First Step (left panel) and the Second Step (right panel) in the step-feed full-scale WWTP, i.e., the nitrifier dinitrification pathway, the NH_2OH pathway and the heterotrophic denitrification pathway (Ni et al., 2015).

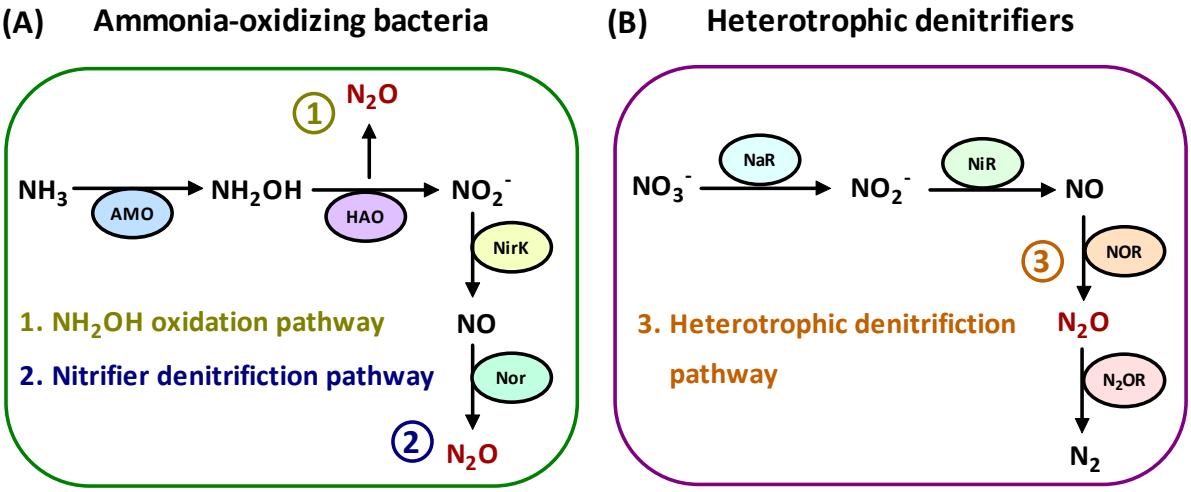

Figure 1. Simplified representation of the three N_2O production pathways by ammonia oxidizing bacteria (A) and heterotrophic denitrifiers (B): nitrifier denitrification, NH_2OH oxidation and heterotrophic denitrification pathways.

ACCEPTED MANUSCRIPT

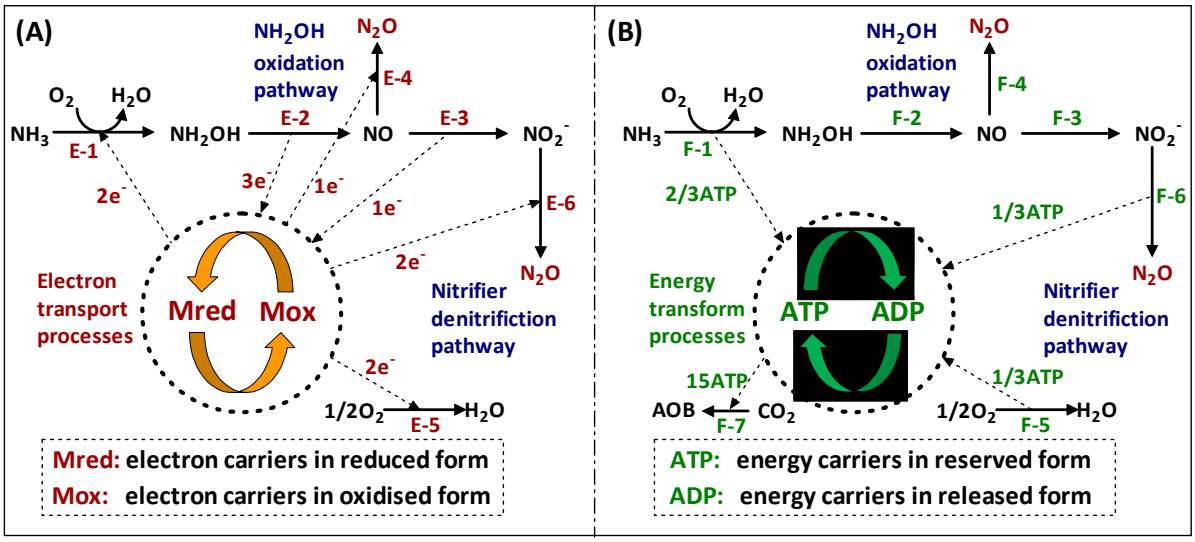

Figure 2. Simplified representation of the electron transfer and energy transform processes in the biochemical reactions (reaction numbers refer to Table S3 in SI) associated with N_2O production by AOB via the two production pathways: (A) Electron balance (Ni et al., 2014), and (B) Energy balance (Peng et al., 2015a).

ACCEPTED MANUSCRIPT

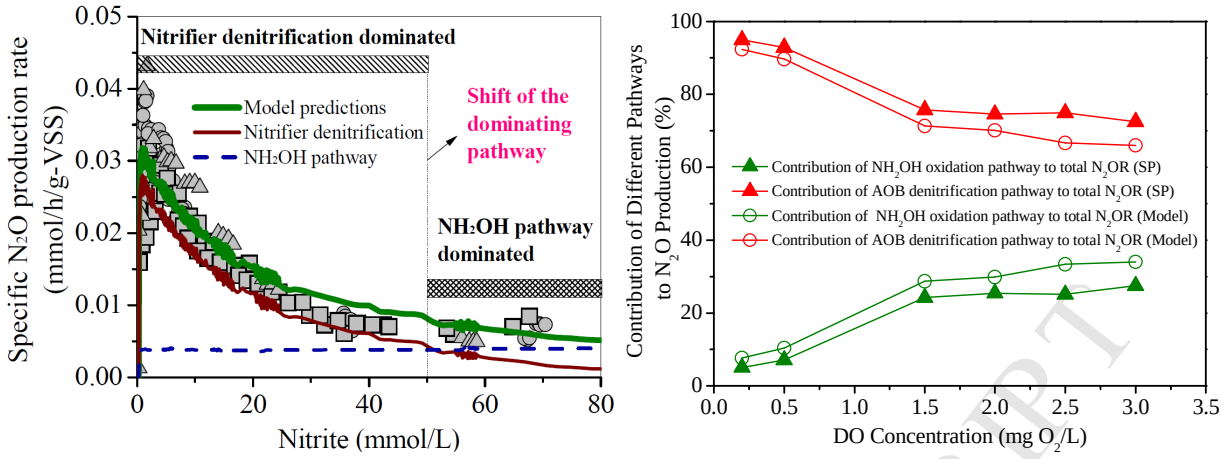

Figure 3. The predicted contributions from the nitrifier dinitrification pathway and the NH_2OH pathway as well as their shifts using Model E (real data: symbols, model predictions: lines) for a partial nitrification (left panel adapted from Ni et al., 2014) and a full nitrification system (right panel adapted from Peng et al., 2014).

ACCEPTED MANUSCRIPT

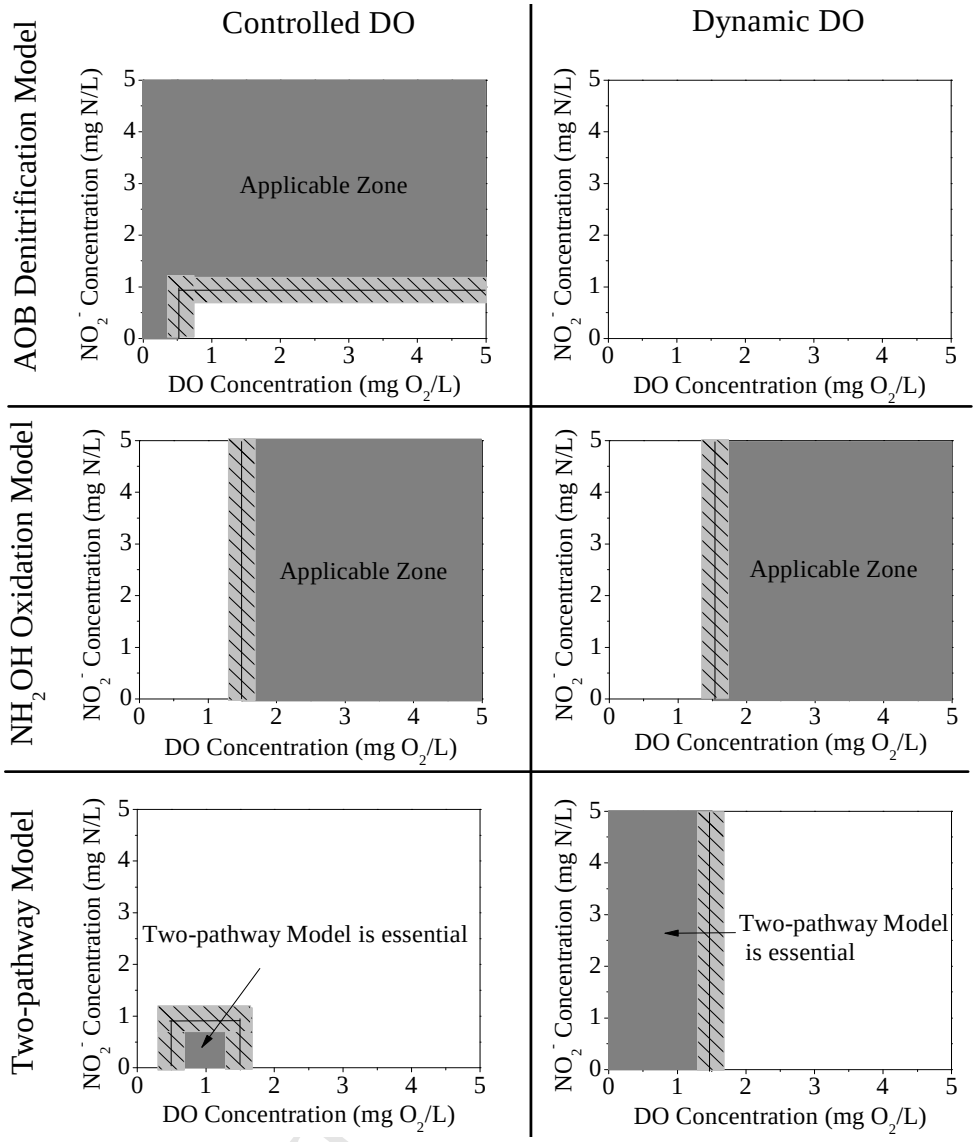

Figure 4. Summary of applicable regions for the AOB denitrification model, the NH_2OH oxidation model and the two-pathway model under various DO and NO_2^- concentrations. The applicable regions were insensitive to the variations of key parameters governing N_2O production by the two-pathway model (Peng et al., 2015b).

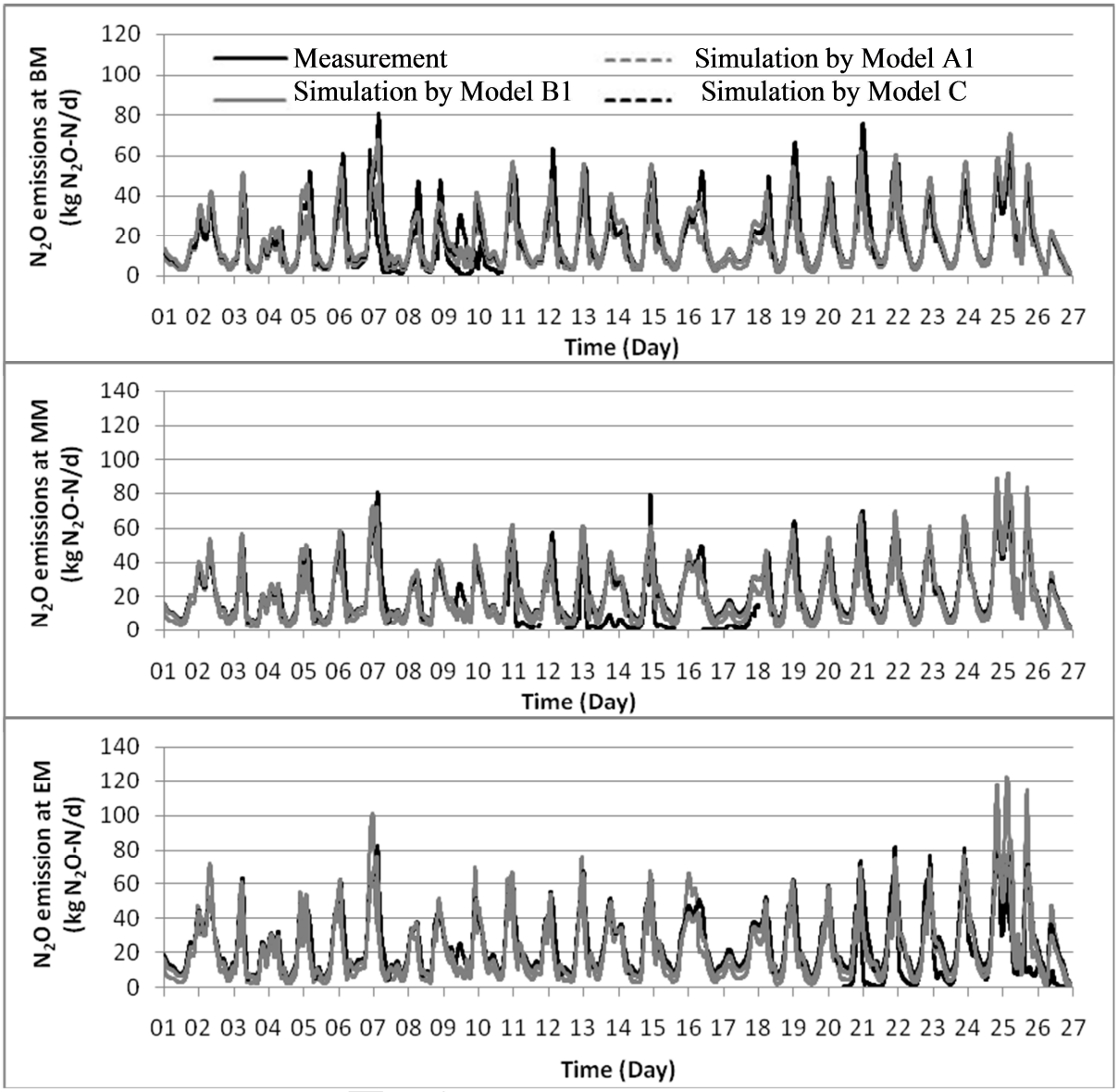

Figure 5. Model evaluation results for N_2O emissions using the measurement results at the beginning (BM) (upper panel), the middle (MM) (middle panel) and the end section (EM) (bottom panel) of the summer aeration package on the UCT process from Eindhoven plant by using ASM-type models that combine one of the single-pathway models of AOB (Models A1, B1 and C) with ASMN (Model G) of heterotrophic denitrifiers (Spérandio et al., 2014).

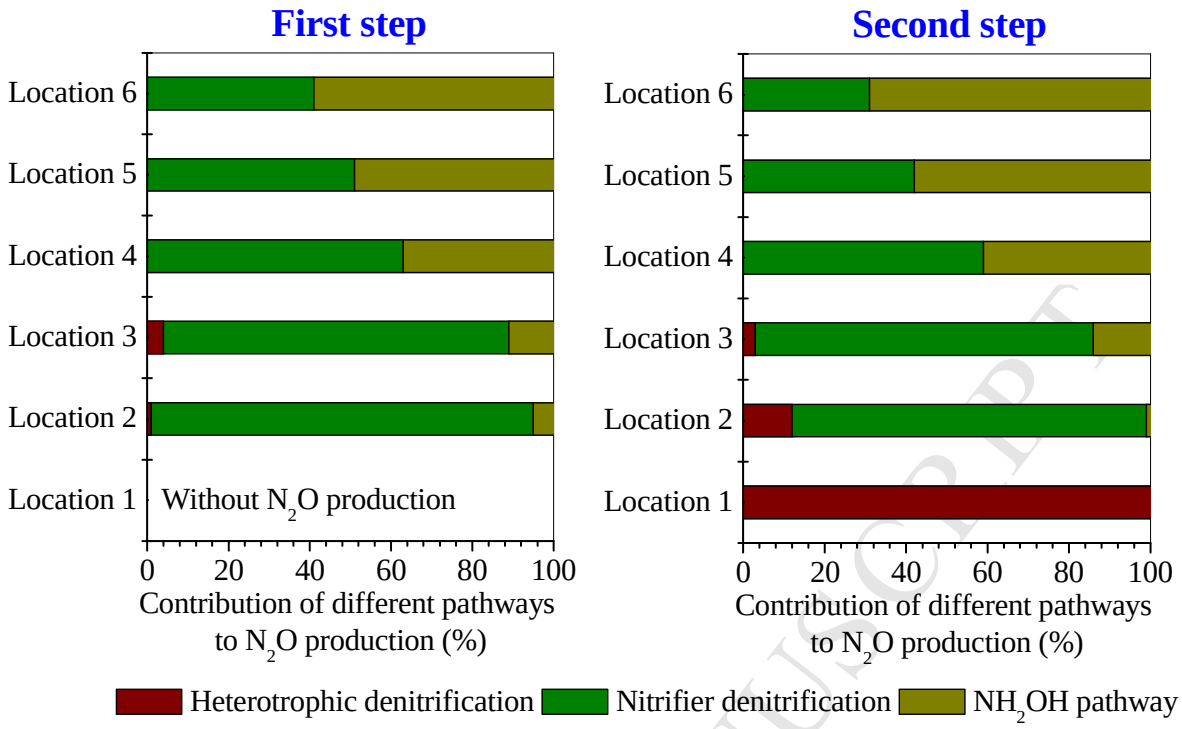

Figure 6. Model predicted percentage contributions from the three N_2O pathways to total N_2O productions at six different locations of the First Step (left panel) and the Second Step (right panel) in the step-feed full-scale WWTP, i.e., the nitrifier dinitrification pathway, the NH_2OH pathway and the heterotrophic denitrification pathway (Ni et al., 2015).

ACCEPTED MANUSCRIPT

ACCEPTED MANUSCRIPT

Highlights

- The models describing all the known microbial pathways for N_2O production are reviewed.
- The N_2O model structures as well as their underlying assumptions are compared.
- Model evaluations using lab-scale and full-scale experimental data are discussed.
- The key kinetic and stoichiometric parameters are summarized and analysed.
- The applicability of these N_2O models under various conditions is elucidated.

ACCEPTED MANUSCRIPT

ACCEPTED MANUSCRIPT

Supplementary Information

Recent Advances in Mathematical Modeling of Nitrous Oxides Emissions from Wastewater Treatment Processes

Bing-Jie Ni,* Zhiguo Yuan

Advanced Water Management Centre, The University of Queensland, St. Lucia, Brisbane, Queensland 4072, Australia

***Corresponding author:**

Dr. Bing-Jie Ni

Advanced Water Management Centre

The University of Queensland

Australia

Phone: + 61 7 3346 3219

Fax: +61 7 3365 4726

E-mail: b.ni@uq.edu.au

The following is included as supplementary information for this paper:

Table S1. The definition of all model components

Variable	Description
S_{O2}	Dissolved oxygen (DO) concentration
S_{NH3}	Ammonia (NH_3) concentration
S_{NH4}	Ammonium (NH_4^+) concentration
S_{NO2}	Nitrite (NO_2^-) concentration
S_{NO3}	Nitrate (NO_3^-) concentration
S_{N2}	Nitrogen gas (N_2) concentration
S_{HNO2}	Free nitrite acid (FNA) concentration
S_{NO}	Nitric oxide (NO) concentration
S_{N2O}	Nitrous oxide (N_2O) concentration
S_{NH2OH}	Hydroxylamine (NH_2OH) concentration
S_{NOH}	Nitrosyl radical (NOH) concentration
S_{Mred}	Reduced form of electron carrier (Mred) concentration
S_{Mox}	Oxidized form of electron carrier (Mox) concentration
S_{ADP}	Released form of energy carrier (ADP) concentration
S_{ATP}	Reserved form of energy carrier (ATP) concentration
S_{CO2}	Inorganic carbon (IC) concentration
S_S	Readily biodegradable COD concentration
X_H	Heterotrophic denitrifiers (HD) concentration
X_{AOB}	Ammonia-oxidizing bacteria (AOB) concentration

Table S2. Process matrices for the six single-pathway N_2O models of AOB in literature

Process	Model Components								Kinetic rate expressions
	S_{O2}	S_{NH4} (S_{NH3})	S_{NH2OH}	S_{NOH}	S_{NO2} (S_{HNO2})	S_{NO}	S_{N2O}	X_{AOB}	
Model A – AOB denitrification pathway (Ni et al., 2011)									
A-1	-1.14	-1	1						$\mu_{AOB,AMO}\frac{S_{O2}}{K_{O2,AOB,1}+S_{O2}}\frac{S_{NH4}}{K_{NH4,AOB}+S_{NH4}}X_{AOB}$
A-2	$-\frac{2.29-Y_{AOB}}{Y_{AOB}}$	$-i_{N,AOB}$	$-\frac{1}{Y_{AOB}}$		$\frac{1}{Y_{AOB}}$			1	$\mu_{AOB,HAO}\frac{S_{O2}}{K_{O2,AOB,2}+S_{O2}}\frac{S_{NH2OH}}{K_{NH2OH,AOB}+S_{NH2OH}}X_{AOB}$
A-3			-1		-3	4			$\eta_{AOB}\mu_{AOB,HAO}\frac{K_{I,O2,AOB}}{S_{O2}+K_{I,O2,AOB}}\frac{S_{NO2}}{K_{NO2,AOB}+S_{NO2}}\frac{S_{NH2OH}}{K_{NH2OH,AOB}+S_{NH2OH}}X_{AOB}$
A-4			-1		1	-4	4		$\eta_{AOB}\mu_{AOB,HAO}\frac{K_{I,O2,AOB}}{S_{O2}+K_{I,O2,AOB}}\frac{S_{NO}}{K_{NO,AOB}+S_{NO}}\frac{S_{NH2OH}}{K_{NH2OH,AOB}+S_{NH2OH}}X_{AOB}$
Model A1 – AOB denitrification pathway (Pocquet et al., 2013)									
A1-1	-1.14	-1	1						$\mu_{AOB,AMO}\frac{S_{O2}}{K_{O2,AOB,1}+S_{O2}}\frac{S_{NH3}}{K_{NH3,AOB}+S_{NH3}+(S_{NH3})^2/K_{I,NH3,AOB}}X_{AOB}$
A1-2	$-\frac{2.29-Y_{AOB}}{Y_{AOB}}$	$-i_{N,AOB}$	$-\frac{1}{Y_{AOB}}$		$\frac{1}{Y_{AOB}}$			1	$\mu_{AOB,HAO}\frac{S_{O2}}{K_{O2,AOB,2}+S_{O2}}\frac{S_{NH2OH}}{K_{NH2OH,AOB}+S_{NH2OH}}X_{AOB}$
A1-3			-1		-3	4			$\eta_{AOB}\mu_{AOB,HAO}\frac{S_{HNO2}}{K_{HNO2,AOB}+S_{HNO2}}\frac{S_{NH2OH}}{K_{NH2OH,AOB}+S_{NH2OH}}X_{AOB}$
A1-4			-1		1	-4	4		$\eta_{AOB}\mu_{AOB,HAO}\frac{S_{NO}}{K_{NO,AOB}+S_{NO}}\frac{S_{NH2OH}}{K_{NH2OH,AOB}+S_{NH2OH}}X_{AOB}$
Model B – AOB denitrification pathway (Mampaey et al., 2013)									
B-1	$-\frac{3.43-Y_{AOB}}{Y_{AOB}}$	$-\frac{1}{Y_{AOB}}-i_{N,AOB}$			$\frac{1}{Y_{AOB}}$			1	$\mu_{AOB}\frac{S_{O2}}{K_{O2,AOB}+S_{O2}}\frac{S_{NH3}}{K_{NH3,AOB}+S_{NH3}}X_{AOB}$
B-2	$-\frac{2.29-Y_{AOB,den}}{Y_{AOB,den}}$	$-\frac{1}{Y_{AOB,den}}-i_{N,AOB}$			$-\frac{1}{Y_{AOB,den}}$	$\frac{2}{Y_{AOB,den}}$		1	$\eta_{AOB}\mu_{AOB}\frac{S_{O2}}{K_{O2,AOB}+S_{O2}}\frac{S_{NH3}}{K_{NH3,AOB}+S_{NH3}}\frac{S_{HNO2}}{K_{HNO2,AOB}+S_{HNO2}}X_{AOB}$
B-3	$-\frac{2.29-Y_{AOB,den}}{Y_{AOB,den}}$	$-\frac{1}{Y_{AOB,den}}-i_{N,AOB}$			$\frac{1}{Y_{AOB,den}}$	$-\frac{2}{Y_{AOB,den}}$	$\frac{2}{Y_{AOB,den}}$	1	$\eta_{AOB}\mu_{AOB}\frac{S_{O2}}{K_{O2,AOB}+S_{O2}}\frac{S_{NH3}}{K_{NH3,AOB}+S_{NH3}}\frac{S_{NO}}{K_{NO,AOB}+S_{NO}}X_{AOB}$

Model B1 – AOB denitrification pathway (Guo and Vanrolleghem, 2014)								
B1-1	$-\frac{3.43-Y_{AOB}}{Y_{AOB}}$	$-\frac{1}{Y_{AOB}}-i_{N,AOB}$			$\frac{1}{Y_{AOB}}$		1	$\mu_{AOB}\frac{S_{O2}}{K_{O2,AOB}+S_{O2}}\frac{S_{NH3}}{K_{NH3,AOB}+S_{NH3}+(S_{NH3})^2/K_{I,NH3,AOB}}\frac{K_{I,HNO2,AOB}}{K_{I,HNO2,AOB}+S_{HNO2}}X_{AOB}$
B1-2	$-\frac{2.29-Y_{AOB,den}}{Y_{AOB,den}}$	$-\frac{1}{Y_{AOB,den}}-i_{N,AOB}$			$-\frac{1}{Y_{AOB,den}}$	$\frac{2}{Y_{AOB,den}}$	1	$\eta_{AOB}\mu_{AOB}\frac{S_{NH3}}{K_{NH3,AOB,den}+S_{NH3}}\frac{S_{HNO2}}{K_{HNO2,AOB}+S_{HNO2}}X_{AOB}DO_{Haldane}$
B1-3	$-\frac{2.29-Y_{AOB,den}}{Y_{AOB,den}}$	$-\frac{1}{Y_{AOB,den}}-i_{N,AOB}$			$\frac{1}{Y_{AOB,den}}$	$-\frac{2}{Y_{AOB,den}}$ $\frac{2}{Y_{AOB,den}}$	1	$\eta_{AOB}\mu_{AOB}\frac{S_{NH3}}{K_{NH3,AOB,den}+S_{NH3}}\frac{S_{NO}}{K_{NO,AOB}+S_{NO}}X_{AOB}DO_{Haldane}$
								$DO_{Haldane}=\frac{S_{O2}}{K_{O2,AOB,den}+(1-2\sqrt{K_{O2,AOB,den}/K_{I,O2,AOB}})S_{O2}+(S_{O2})^2/K_{I,O2,AOB}}$
Model C – NH_2OH/NOH pathway (Law et al., 2012)								
C-1	-1.14	-1	1					$\mu_{AOB,AMO}\frac{S_{O2}}{K_{O2,AOB,1}+S_{O2}}\frac{S_{NH4}}{K_{NH4,AOB}+S_{NH4}}X_{AOB}$
C-2	$-\frac{1.14-Y_{AOB}}{Y_{AOB}}$	$-i_{N,AOB}$	$-\frac{1}{Y_{AOB}}$	$\frac{1}{Y_{AOB}}$			1	$\mu_{AOB,HAO,1}\frac{S_{O2}}{K_{O2,AOB,2}+S_{O2}}\frac{S_{NH2OH}}{K_{NH2OH,AOB}+S_{NH2OH}}X_{AOB}$
C-3	-1.14			-1	1			$\mu_{AOB,HAO,2}\frac{S_{O2}}{K_{O2,AOB,2}+S_{O2}}\frac{S_{NOH}}{K_{NOH,AOB}+S_{NOH}}X_{AOB}$
C-4				-1			1	$k_{NOH}S_{NOH}$
Model D – NH_2OH/NO pathway (Ni et al., 2013b)								
D-1	-1.14	-1	1					$\mu_{AOB,AMO}\frac{S_{O2}}{K_{O2,AOB,1}+S_{O2}}\frac{S_{NH4}}{K_{NH4,AOB}+S_{NH4}}X_{AOB}$
D-2	$-\frac{1.71-Y_{AOB}}{Y_{AOB}}$	$-i_{N,AOB}$	$-\frac{1}{Y_{AOB}}$			$\frac{1}{Y_{AOB}}$	1	$\mu_{AOB,HAO,1}\frac{S_{O2}}{K_{O2,AOB,2}+S_{O2}}\frac{S_{NH2OH}}{K_{NH2OH,AOB}+S_{NH2OH}}X_{AOB}$
D-3	-0.57			1	-1			$\mu_{AOB,HAO,2}\frac{S_{O2}}{K_{O2,AOB,2}+S_{O2}}\frac{S_{NO}}{K_{NO,AOB}+S_{NO}}X_{AOB}$
D-4			-1	1	-4	4		$\eta_{AOB}\mu_{AOB,HAO,1}\frac{S_{NO}}{K_{NO,AOB}+S_{NO}}\frac{S_{NH2OH}}{K_{NH2OH,AOB}+S_{NH2OH}}X_{AOB}$

Table S3. Process matrices for the two two-pathway N_2O models of AOB in literature

Process	Model Components												Kinetic rate expressions
	S_{O2}	S_{NH3}	S_{NH2OH}	S_{NO2}	S_{NO}	S_{N2O}	S_{Mox}	S_{Mred}	S_{ADP}	S_{ATP}	S_{CO2}	X_{AOB}	
Model E – Decoupling approach, electron balance based model (Ni et al., 2014)													
E-1	-1	-1	1				1	-1					$r_{NH3,ox}\frac{S_{O2}}{K_{O2,NH3}+S_{O2}}\frac{S_{NH3}}{K_{NH3}+S_{NH3}}\frac{S_{Mred}}{K_{Mred,1}+S_{Mred}}X_{AOB}$
E-2			-1		1		-3/2	3/2					$r_{NH2OH,ox}\frac{S_{NH2OH}}{K_{NH2OH}+S_{NH2OH}}\frac{S_{Mox}}{K_{Mox}+S_{Mox}}X_{AOB}$
E-3				1	-1		-1/2	1/2					$r_{NO,ox}\frac{S_{NO}}{K_{NO,ox}+S_{NO}}\frac{S_{Mox}}{K_{Mox}+S_{Mox}}X_{AOB}$
E-4					-1	1/2	1/2	-1/2					$r_{NO,red}\frac{S_{NO}}{K_{NO,red}+S_{NO}}\frac{S_{Mred}}{K_{Mred,2}+S_{Mred}}X_{AOB}$
E-5	-1/2						1	-1					$r_{O2,red}\frac{S_{O2}}{K_{O2,red}+S_{O2}}\frac{S_{Mred}}{K_{Mred,3}+S_{Mred}}X_{AOB}$
E-6				-1		1/2	1	-1					$r_{NO2,red}\frac{S_{NO2}}{K_{NO2}+S_{NO2}}\frac{S_{Mred}}{K_{Mred,4}+S_{Mred}}X_{AOB}$
													$S_{Mred}+S_{Mox}=C_{tot}$
Model F – Decoupling approach, electron and ATP balance based model (Peng et al., 2015a)													
F-1	-1	-1	1				1	-1	-2/3	2/3			$r_{NH3,ox}\frac{S_{O2}}{K_{O2,NH3}+S_{O2}}\frac{S_{NH3}}{K_{NH3}+S_{NH3}}\frac{S_{Mred}}{K_{Mred,1}+S_{Mred}}\frac{S_{ADP}}{K_{ADP}+S_{ADP}}X_{AOB}$
F-2			-1		1		-1	1					$r_{NH2OH,ox}\frac{S_{NH2OH}}{K_{NH2OH}+S_{NH2OH}}\frac{S_{Mox}}{K_{Mox}+S_{Mox}}X_{AOB}$
F-3				1	-1		-1	1					$r_{NO,ox}\frac{S_{NO}}{K_{NO,ox}+S_{NO}}\frac{S_{Mox}}{K_{Mox}+S_{Mox}}X_{AOB}$
F-4					-1	1/2							$r_{NO,red}S_{NO}$

ACCEPTED MANUSCRIPT

F-5	-1/2				1	-1	-1/3	1/3		$r_{O2,red}\frac{S_{O2}}{K_{O2,red}+S_{O2}}\frac{S_{Mred}}{K_{Mred,2}+S_{Mred}}\frac{S_{ADP}}{K_{ADP}+S_{ADP}}X_{AOB}$
F-6		-1		1/2	1	-1	-1/3	1/3		$r_{NO2,red}\frac{S_{NO2}}{K_{NO2}+S_{NO2}}\frac{S_{Mred}}{K_{Mred,3}+S_{Mred}}\frac{S_{ADP}}{K_{ADP}+S_{ADP}}X_{AOB}$
F-7					2	-2	15	-15	-1	1	$r_{AOB}\frac{S_{CO2}}{K_{CO2}+S_{CO2}}\frac{S_{Mred}}{K_{Mred,4}+S_{Mred}}\frac{S_{ATP}}{K_{ATP}+S_{ATP}}X_{AOB}$
										$S_{Mred}+S_{Mox}=C_{tot,1}$
										$S_{ADP}+S_{ATP}=C_{tot,2}$

ACCEPTED MANUSCRIPT

Table S4. Process matrices for the two types of four-step denitrification models describing N_2O production by heterotrophic denitrifiers

Process	Model Components									Kinetic rate expressions
	S_{NO3}	S_{NO2}	S_{NO}	S_{N2O}	S_{N2}	S_S	S_{Mox}	S_{Mred}	X_H	
Model G – ASMN, the "direct coupling approach" adapted from Hiatt and Grady (2008)										
G-1	$-\frac{1-Y_H\cdot\eta_Y}{1.143\cdot Y_H\cdot\eta_Y}$	$\frac{1-Y_H\cdot\eta_Y}{1.143\cdot Y_H\cdot\eta_Y}$				$-1/(Y_H\cdot\eta_Y)$			1	$\mu_H\eta_{g1}(\frac{S_S}{K_{S1}+S_S})(\frac{S_{NO3}}{K_{NO3}^{HB}+S_{NO3}})X_H$
G-2		$-\frac{1-Y_H\cdot\eta_Y}{0.571\cdot Y_H\cdot\eta_Y}$	$\frac{1-Y_H\cdot\eta_Y}{0.571\cdot Y_H\cdot\eta_Y}$			$-1/(Y_H\cdot\eta_Y)$			1	$\mu_H\eta_{g2}(\frac{S_S}{K_{S2}+S_S})(\frac{S_{NO2}}{K_{NO2}^{HB}+S_{NO2}})(\frac{K_{NO,2}}{K_{NO,2}+S_{NO}})X_H$
G-3			$-\frac{1-Y_H\cdot\eta_Y}{0.571\cdot Y_H\cdot\eta_Y}$	$\frac{1-Y_H\cdot\eta_Y}{0.571\cdot Y_H\cdot\eta_Y}$		$-1/(Y_H\cdot\eta_Y)$			1	$\mu_H\eta_{g3}(\frac{S_S}{K_{S3}+S_S})(\frac{S_{NO}}{K_{NO}^{HB}+S_{NO}+S_{NO}^2/K_{NO,3}})X_H$
G-4				$-\frac{1-Y_H\cdot\eta_Y}{0.571\cdot Y_H\cdot\eta_Y}$	$\frac{1-Y_H\cdot\eta_Y}{0.571\cdot Y_H\cdot\eta_Y}$	$-1/(Y_H\cdot\eta_Y)$			1	$\mu_H\eta_{g4}(\frac{S_S}{K_{S4}+S_S})(\frac{S_{N2O}}{K_{N2O}^{HB}+S_{N2O}})(\frac{K_{NO,4}}{K_{NO,4}+S_{NO}})X_H$
Model H – ASM-ICE, the "indirect coupling approach" adapted from Pan et al. (2013b)										
H-1						-1	$-(1-Y_H)$	$1-Y_H$	Y_H	$r_{COD,\max}(\frac{S_S}{K_S+S_S})(\frac{S_{Mox}}{K_{Mox}+S_{Mox}})X_H$
H-2	-1	1					1	-1		$r_{NO3,\max}(\frac{S_{NO3}}{K_{NO3}^{HB}+S_{NO3}})(\frac{S_{Mred}}{K_{Mred,1}+S_{Mred}})X_H$
H-3		-1	1				$\frac{1}{2}$	$-\frac{1}{2}$		$r_{NO2,\max}(\frac{S_{NO2}}{K_{NO2}^{HB}+S_{NO2}})(\frac{S_{Mred}}{K_{Mred,2}+S_{Mred}})X_H$
H-4			-1	$\frac{1}{2}$			$\frac{1}{2}$	$-\frac{1}{2}$		$r_{NO,\max}(\frac{S_{NO}}{K_{NO}^{HB}+S_{NO}})(\frac{S_{Mred}}{K_{Mred,3}+S_{Mred}})X_H$
H-5				-1	1		1	-1		$r_{N2O,\max}(\frac{S_{N2O}}{K_{N2O}^{HB}+S_{N2O}})(\frac{S_{Mred}}{K_{Mred,4}+S_{Mred}})X_H$
										$S_{Mred}+S_{Mox}=C_{tot}$

Table S5. Kinetic and stoichiometric parameters of all the N_2O models reviewed

Parameter	Definition	Typical values	Source
Model A – AOB denitrification pathway			
Y_{AOB}	Yield coefficient for AOB, g COD g^{-1} N	0.150	Ni et al. (2011)
$i_{N,AOB}$	Nitrogen content of biomass, g N g-1 COD	0.07	Ni et al. (2011)
$\mu_{AOB,AMO}$	Maximum AMO-mediated reaction rate, h^{-1}	0.122	Ni et al. (2011)
$\mu_{AOB,HAO}$	Maximum HAO-mediated reaction rate, h^{-1}	0.092	Ni et al. (2011)
$K_{O2,AOB,1}$	S_{O2} affinity constant for S_{NH4} oxidation, g DO m^{-3}	0.043	Ni et al. (2011)
$K_{O2,AOB,2}$	S_{O2} affinity constant for S_{NH2OH} oxidation, g DO m^{-3}	0.6	Ni et al. (2011)
$K_{I,O2,AOB}$	S_{O2} substrate inhibition parameter, g DO m^{-3}	0.112	Ni et al. (2011)
η_{AOB}	Anoxic reduction factor	0.074	Ni et al. (2011)
$K_{NH4,AOB}$	S_{NH4} affinity constant for AOB, g N m^{-3}	2.4	Ni et al. (2011)
$K_{NH2OH,AOB}$	S_{NH2OH} affinity constant for AOB, g N m^{-3}	2.4	Ni et al. (2011)
$K_{NO2,AOB}$	S_{NO2} affinity constant for AOB, g N m^{-3}	0.14	Ni et al. (2011)
$K_{NO,AOB}$	S_{NO} affinity constant for AOB, g N m^{-3}	0.0084	Ni et al. (2011)
Model A1 – AOB denitrification pathway			
Y_{AOB}	Yield coefficient for AOB, g COD g^{-1} N	0.150	Pocquet et al. (2013)
$i_{N,AOB}$	Nitrogen content of biomass, g N g-1 COD	0.07	Pocquet et al. (2013)
$\mu_{AOB,AMO}$	Maximum AMO-mediated reaction rate, h^{-1}	0.216	Pocquet et al. (2013)
$\mu_{AOB,HAO}$	Maximum HAO-mediated reaction rate, h^{-1}	0.062	Pocquet et al. (2013)
$K_{O2,AOB,1}$	S_{O2} affinity constant for S_{NH4} oxidation, g DO m^{-3}	0.043	Pocquet et al. (2013)
$K_{O2,AOB,2}$	S_{O2} affinity constant for S_{NH2OH} oxidation, g DO m^{-3}	0.6	Pocquet et al. (2013)
η_{AOB}	Anoxic reduction factor	0.20	Pocquet et al. (2013)
$K_{NH3,AOB}$	S_{NH3} affinity constant for AOB, g N m^{-3}	0.4575	Pocquet et al. (2013)
$K_{I,NH3,AOB}$	S_{NH3} substrate inhibition constant for AOB, g N m^{-3}	16	Pocquet et al. (2013)

$K_{NH2OH,AOB}$	S_{NH2OH} affinity constant for AOB, g N m^{-3}	2.4	Pocquet et al. (2013)
$K_{HNO2,AOB}$	S_{HNO2} affinity constant for AOB, g N m^{-3}	0.002	Pocquet et al. (2013)
$K_{NO,AOB}$	S_{NO} affinity constant for AOB, g N m^{-3}	0.004	Pocquet et al. (2013)
Model B – AOB denitrification pathway			
Y_{AOB}	Yield coefficient for AOB, g COD g^{-1} N	0.150	Mampaey et al. (2013)
$i_{N,AOB}$	Nitrogen content of biomass, g N g^{-1} COD	0.07	Mampaey et al. (2013)
μ_{AOB}	Maximum AOB growth rate, h^{-1}	0.045	Mampaey et al. (2013)
η_{AOB}	Anoxic reduction factor	0.03	Mampaey et al. (2013)
$K_{NH3,AOB}$	S_{NH3} affinity constant for AOB, g N m^{-3}	1.0	Mampaey et al. (2013)
$K_{NO,AOB}$	S_{NO} affinity constant for AOB, g DO m^{-3}	1.0	Mampaey et al. (2013)
$K_{HNO2,AOB}$	S_{HNO2} affinity constant for AOB, g N m^{-3}	0.002	Mampaey et al. (2013)
$K_{O2,AOB}$	S_{O2} affinity constant for AOB, g DO m^{-3}	0.5	Mampaey et al. (2013)
Model B1 – AOB denitrification pathway			
Y_{AOB}	Yield coefficient for AOB, g COD g^{-1} N	0.180	Guo and Vanrolleghem (2014)
$Y_{AOB,den}$	Yield coefficient for AOB denitrification, g COD g^{-1} N	0.150	Guo and Vanrolleghem (2014)
$i_{N,AOB}$	Nitrogen content of biomass, g N g-1 COD	0.07	Guo and Vanrolleghem (2014)
μ_{AOB}	Maximum AOB growth rate, h^{-1}	0.032	Guo and Vanrolleghem (2014)
η_{AOB}	Anoxic reduction factor	0.3	Guo and Vanrolleghem (2014)
$K_{NH3,AOB}$	S_{NH3} affinity constant for AOB, g N m^{-3}	0.007	Guo and Vanrolleghem (2014)
$K_{NH3,AOB,den}$	S_{NH3} affinity constant for AOB denitrification, g N m^{-3}	0.0041	Guo and Vanrolleghem (2014)
$K_{I,NH3,AOB}$	S_{NH3} substrate inhibition constant for AOB, g N m^{-3}	0.1	Guo and Vanrolleghem (2014)
$K_{NO,AOB}$	S_{NO} affinity constant for AOB, g DO m^{-3}	0.1	Guo and Vanrolleghem (2014)
$K_{HNO2,AOB}$	S_{HNO2} affinity constant for AOB, g N m^{-3}	0.00001	Guo and Vanrolleghem (2014)
$K_{I,HNO2,AOB}$	S_{HNO2} inhibition constant for AOB, g N m^{-3}	0.001	Guo and Vanrolleghem (2014)

$K_{O2,AOB}$	S_{O2} affinity constant for AOB, g DO m^{-3}	0.6	Guo and Vanrolleghem (2014)
$K_{O2,AOB,den}$	S_{O2} affinity constant for AOB denitrification, g m^{-3}	2.14	Guo and Vanrolleghem (2014)
$K_{I,O2,AOB}$	S_{O2} substrate inhibition parameter, g DO m^{-3}	4.68	Guo and Vanrolleghem (2014)
Model C – AOB NH_2OH/NOH pathway			
Y_{AOB}	Yield coefficient for AOB, g COD g^{-1} N	0.150	Law et al. (2012)
$i_{N,AOB}$	Nitrogen content of biomass, g N g-1 COD	0.07	Law et al. (2012)
$\mu_{AOB,AMO}$	Maximum AMO-mediated reaction rate, h^{-1}	0.205	Law et al. (2012)
$\mu_{AOB,HAO,1}$	Maximum HAO-mediated reaction rate for NH_2OH oxidation, h^{-1}	0.065	Law et al. (2012)
$\mu_{AOB,HAO,2}$	Maximum HAO-mediated reaction rate for NOH oxidation, h^{-1}	0.43	Law et al. (2012)
$K_{S1,O2\_AOB}$	S_{O2} affinity constant for S_{NH4} oxidation, g DO m^{-3}	0.4	Law et al. (2012)
$K_{S2,O2\_AOB}$	S_{O2} affinity constant for S_{NH2OH} oxidation, g DO m^{-3}	0.056	Law et al. (2012)
k_{NOH}	Maximum reaction rate for NOH decomposition, h^{-1}	0.79	Law et al. (2012)
$K_{NH4,AOB}$	S_{NH4} affinity constant for AOB, g N m^{-3}	2.4	Law et al. (2012)
$K_{NH2OH,AOB}$	S_{NH2OH} affinity constant for AOB, g N m^{-3}	0.7	Law et al. (2012)
$K_{NOH,AOB}$	S_{NOH} affinity constant for AOB, g N m^{-3}	0.7	Law et al. (2012)
Model D – AOB NH_2OH/NO pathway			
Y_{AOB}	Yield coefficient for AOB, g COD g^{-1} N	0.150	Ni et al. (2013b)
$i_{N,AOB}$	Nitrogen content of biomass, g N g-1 COD	0.07	Ni et al. (2013b)
$\mu_{AOB,AMO}$	Maximum AMO-mediated reaction rate, h^{-1}	0.205	Ni et al. (2013b)
$\mu_{AOB,HAO,1}$	Maximum HAO-mediated reaction rate for NH_2OH oxidation, h^{-1}	0.085	Ni et al. (2013b)
$\mu_{AOB,HAO,2}$	Maximum HAO-mediated reaction rate for NOH oxidation, h^{-1}	0.567	Ni et al. (2013b)
$K_{S1,O2\_AOB}$	S_{O2} affinity constant for S_{NH4} oxidation, g DO m^{-3}	0.4	Ni et al. (2013b)
$K_{S2,O2\_AOB}$	S_{O2} affinity constant for S_{NH2OH} oxidation, g DO m^{-3}	0.073	Ni et al. (2013b)
η_{AOB}	Anoxic reduction factor	0.285	Ni et al. (2013b)

$K_{NH4,AOB}$	S_{NH4} affinity constant for AOB, g N m^{-3}	2.4	Ni et al. (2013b)
$K_{NH2OH,AOB}$	S_{NH2OH} affinity constant for AOB, g N m^{-3}	2.4	Ni et al. (2013b)
$K_{NO,AOB}$	S_{NO} affinity constant for AOB, g N m^{-3}	0.0084	Ni et al. (2013b)
Model E – Two-pathway model of AOB			
$r_{NH3,ox}$	Specific maximum ammonia oxidation rate, mmol/(g-VSS*h)	14.75	Ni et al. (2014)
$r_{NH2OH,ox}$	Specific maximum NH_2OH oxidation rate, mmol/(g-VSS*h)	22.86	Ni et al. (2014)
$r_{NO,ox}$	Specific maximum NO oxidation rate, mmol/(g-VSS*h)	22.86	Ni et al. (2014)
$r_{O2,red}$	Specific maximum oxygen reduction rate, mmol/(g-VSS*h)	48.02	Ni et al. (2014)
$r_{NO2,red}$	Specific maximum nitrite reduction rate, mmol/(g-VSS*h)	3.06	Ni et al. (2014)
$r_{NO,red}$	Specific maximum NO reduction rate, mmol/(g-VSS*h)	1.6×10^{-2}	Ni et al. (2014)
$K_{O2,NH3}$	Oxygen affinity constant for ammonia oxidation, mmol-O_2/L	1.9×10^{-2}	Ni et al. (2014)
K_{NH3}	Ammonia affinity constant for ammonia oxidation, mmol-N/L	1.7×10^{-1}	Ni et al. (2014)
K_{NH2OH}	NH_2OH affinity constant for NH_2OH oxidation, mmol-N/L	5×10^{-2}	Ni et al. (2014)
$K_{NO,ox}$	NO affinity constant for NO oxidation, mmol-N/L	6×10^{-4}	Ni et al. (2014)
$K_{O2,red}$	Oxygen affinity constant for oxygen reduction, mmol-O_2/L	1.9×10^{-3}	Ni et al. (2014)
K_{NO2}	Nitrite affinity constant for nitrite reduction, mmol-N/L	1×10^{-2}	Ni et al. (2014)
$K_{NO,red}$	NO affinity constant for NO reduction, mmol-N/L	6×10^{-4}	Ni et al. (2014)
K_{Mox}	S_{Mox} affinity constant for NH_2OH or NO oxidation, mmol/g-VSS	$1\times10^{-2}\times C_{tot}$	Ni et al. (2014)
$K_{Mred,1}$	S_{Mred} affinity constant for ammonia oxidation, mmol/g-VSS	$1\times10^{-3}\times C_{tot}$	Ni et al. (2014)
$K_{Mred,2}$	S_{Mred} affinity constant for NO reduction, mmol/g-VSS	$1\times10^{-3}\times C_{tot}$	Ni et al. (2014)
$K_{Mred,3}$	S_{Mred} affinity constant for oxygen reduction, mmol/g-VSS	6.9×10^{-2}	Ni et al. (2014)
$K_{Mred,4}$	S_{Mred} affinity constant for nitrite reduction, mmol/g-VSS	1.9×10^{-1}	Ni et al. (2014)
C_{tot}	The sum of S_{Mred} and S_{Mox}, an assumed constant, mmol/g-VSS	1×10^{-2}	Ni et al. (2014)
Model F – Two-pathway model of AOB			
$r_{NH3,ox}$	Maximum ammonia oxidation rate, mmol/(g-VSS*h)	14.75	Peng et al. (2015a)

$r_{NH2OH,ox}$	Maximum NH_2OH oxidation rate, mmol/(g-VSS*h)	22.86	Peng et al. (2015a)
$r_{NOH,ox}$	Maximum NOH oxidation rate, mmol/(g-VSS*h)	13.42	Peng et al. (2015a)
$r_{O2,red}$	Maximum oxygen reduction rate, mmol/(g-VSS*h)	48.02	Peng et al. (2015a)
$r_{NO2,red}$	Maximum nitrite reduction rate, mmol/(g-VSS*h)	3.06	Peng et al. (2015a)
$r_{NO,red}$	Maximum NOH decomposition rate, mmol/(mmol*h)	6×10^{-2}	Peng et al. (2015a)
r_{AOB}	Maximum AOB growth rate with CO2 fixation, mmol/(g-VSS*h)	1.55	Peng et al. (2015a)
$K_{O2,NH3}$	Oxygen affinity constant for ammonia oxidation, mmol-O_2/L	1.9×10^{-2}	Peng et al. (2015a)
K_{NH3}	Ammonia affinity constant for ammonia oxidation, mmol-N/L	1.7×10^{-1}	Peng et al. (2015a)
K_{NH2OH}	NH_2OH affinity constant for NH_2OH oxidation, mmol-N/L	5×10^{-2}	Peng et al. (2015a)
$K_{NOH,ox}$	NOH affinity constant for NOH oxidation, mmol-N/L	5×10^{-2}	Peng et al. (2015a)
$K_{O2,red}$	Oxygen affinity constant for oxygen reduction, mmol-O_2/L	1.9×10^{-3}	Peng et al. (2015a)
K_{NO2}	Nitrite affinity constant for nitrite reduction, mmol-N/L	1×10^{-2}	Peng et al. (2015a)
K_{CO2}	CO_2 affinity constant for carbon fixation, mmol-C/L	2.35	Peng et al. (2015a)
K_{Mox}	S_{Mox} affinity constant for NH_2OH and NOH oxidation, mmol/g-VSS	2.1×10^{-2}	Peng et al. (2015a)
$K_{Mred,1}$	S_{Mred} affinity constant for ammonia oxidation, mmol/g-VSS	$1\times10^{-3}\times C_{tot}$	Peng et al. (2015a)
$K_{Mred,2}$	S_{Mred} affinity constant for oxygen reduction, mmol/g-VSS	6.9×10^{-3}	Peng et al. (2015a)
$K_{Mred,3}$	S_{Mred} affinity constant for nitrite reduction, mmol/g-VSS	8.2×10^{-3}	Peng et al. (2015a)
$K_{Mred,4}$	S_{Mred} affinity constant for cell growth, mmol/g-VSS	$1\times10^{-3}\times C_{tot}$	Peng et al. (2015a)
K_{ATP}	S_{ATP} affinity constant for cell growth, mmol/g-VSS	4.4×10^{-3}	Peng et al. (2015a)
K_{ADP}	S_{ADP} affinity constant for ammonia oxidation, mmol/g-VSS	1.44×10^{-2}	Peng et al. (2015a)
$C_{tot,1}$	The sum of S_{Mred} and S_{Mox}, which is a constant, mmol/g-VSS	1×10^{-2}	Peng et al. (2015a)
$C_{tot,2}$	The sum of S_{ADP} and S_{ATP}, which is a constant, mmol/g-VSS	3×10^{-2}	Peng et al. (2015a)
Model G – ASMN of heterotrophic denitrifiers			
μ_H	Maximum specific growth rate, h^{-1}	0.26	Hiatt and Grady (2008)
Y_H	Yield coefficient for heterotrophs, g COD g^{-1} COD	0.6	Hiatt and Grady (2008)

η_Y	Anoxic yield factor, dimensionless	0.9	Hiatt and Grady (2008)
η_{g1}	Anoxic growth factor for nitrate reduction, dimensionless	0.28	Hiatt and Grady (2008)
η_{g2}	Anoxic growth factor for nitrite reduction, dimensionless	0.16	Hiatt and Grady (2008)
η_{g3}	Anoxic growth factor for NO reduction, dimensionless	0.35	Hiatt and Grady (2008)
η_{g4}	Anoxic growth factor for N_2O reduction, dimensionless	0.35	Hiatt and Grady (2008)
K_{S1}	Affinity constant for Ss in nitrate reduction, g-COD m^{-3}	20	Hiatt and Grady (2008)
K_{S2}	Affinity constant for Ss in nitrite reduction, g-COD m^{-3}	20	Hiatt and Grady (2008)
K_{S3}	Affinity constant for Ss in NO reduction, g-COD m^{-3}	20	Hiatt and Grady (2008)
K_{S4}	Affinity constant for Ss in N_2O reduction, g-COD m^{-3}	40	Hiatt and Grady (2008)
K_{NO3}^{HB}	Affinity constant for nitrate, g N m^{-3}	0.2	Hiatt and Grady (2008)
K_{NO2}^{HB}	Affinity constant for nitrite, g N m^{-3}	0.2	Hiatt and Grady (2008)
K_{NO}^{HB}	Affinity constant for NO, g N m^{-3}	0.05	Hiatt and Grady (2008)
K_{N2O}^{HB}	Affinity constant for N_2O, g N m^{-3}	0.05	Hiatt and Grady (2008)
$K_{I,NO,2}$	NO inhibition coefficient for nitrite reduction, g N m^{-3}	0.5	Hiatt and Grady (2008)
$K_{I,NO,3}$	NO inhibition coefficient for NO reduction, g N m^{-3}	0.3	Hiatt and Grady (2008)
$K_{I,NO,4}$	NO inhibition coefficient for N_2O reduction, g N m^{-3}	0.075	Hiatt and Grady (2008)
Model H – ASM-ICE of heterotrophic denitrifiers			
$r_{COD,\max}$	Maximum carbon source oxidation rate, mmol COD/(L*h)	0.34	Pan et al. (2015)
$r_{NO3,\max}$	Maximum nitrate reduction rate, mmol NO_3^-/(mmol biomass*h)	0.045	Pan et al. (2013b)
$r_{NO2,\max}$	Maximum nitrite reduction rate, mmol NO_2^-/(mmol biomass*h)	0.059	Pan et al. (2013b)
$r_{NO,\max}$	Maximum NO reaction rate, mmol NO /(mmol biomass*h)	0.56	Pan et al. (2013b)
$r_{N2O,\max}$	Maximum N_2O reaction rate, mmol N_2O/(mmol biomass*hour)	0.23	Pan et al. (2013b)

K_S	Affinity constant for Ss, mmol COD/L	0.1	Pan et al. (2013b)
K_{NO3}^{HB}	Affinity constant for nitrate, mmol NO_3^- /L	0.018	Pan et al. (2013b)
K_{NO2}^{HB}	Affinity constant for nitrite, mmol NO_2^- /L	0.0041	Pan et al. (2013b)
K_{NO}^{HB}	Affinity constant for NO, mmol NO/L	0.000011	Pan et al. (2013b)
K_{N2O}^{HB}	Affinity constant for N_2O, mmol N_2O/L	0.0025	Pan et al. (2013b)
K_{Mox}	Affinity constant for S_{Mox} for Ss oxidation, mmol/mmol biomass	0.0001	Pan et al. (2013b)
$K_{Mred,1}$	Affinity constant for S_{Mred} in nitrate reduction, mmol/mmol biomass	0.0046	Pan et al. (2013b)
$K_{Mred,2}$	Affinity constant for S_{Mred} in nitrite reduction, mmol/mmol biomass	0.0004	Pan et al. (2013b)
$K_{Mred,3}$	Affinity constant for S_{Mred} in NO reduction, mmol/mmol biomass	0.00001	Pan et al. (2013b)
$K_{Mred,4}$	Affinity constant for S_{Mred} in N_2O reduction, mmol/mmol biomass	0.0032	Pan et al. (2013b)
Y_H	Yield coefficient for heterotrophs, mmol/mmol	0.5	Pan et al. (2013b)
C_{tot}	Total electron carrier concentration, mmol/mmol biomass	0.01	Pan et al. (2013b)

ACCEPTED